Adaptive Facade Using SMP Actuator for Enhancing Thermal Performance in Buildings

Mahmoud Zameem * , Paolo Beccarelli , Christopher Wood

Posted Date: 14 July 2023

doi: 10.20944/preprints202307.0931.v1

Keywords: adaptive facade; shape memory polymer (SMP); actuator; thermoresponsive; building perfro-mance; simulation

Article

Adaptive Facade Using SMP Actuator for Enhancing Thermal Performance in Buildings

Mahmoud Zameem [1,*], Paolo Beccarelli [2] and Christopher Wood [3]

[1] Architecture Researcher, Department of Architecture and Built Environment, University of Nottingham; mahmoud.zameem@nottingham.ac.uk
[2] Associate Professor, Department of Architecture and Built Environment, University of Nottingham; paolo.beccarelli@nottingham.ac.uk
[3] Associate Professor, Department of Architecture and Built Environment, University of Nottingham; christopher.wood@nottingham.ac.uk
* Correspondence: arch.mzameem@gmail.com; Tel.: +447842926658

Abstract: Shape Memory Polymer (SMP) actuators are smart materials that adapt and switch shape in response to environmental conditions, allowing controlled and dynamic building systems. The integrated SMP strip enabled the adaptive facade shading system to operate independently and with flexibility under certain thermoresponsive conditions to regulate building performance. This study aims to improve adaptive façade performance in a hot-humid climate by determining optimal thermal activation factors for the shape memory polymer. This was achieved by comprehensively examining and analysing the impact of various SMP activation parameters on energy efficiency, thermal comfort, and visual comfort. In addition, dynamic IES-VE building energy simulation was used to evaluate the thermal performance of the adaptable facade. The results were validated using a multicriteria approach to compare with the existing glass façade of a high-rise apartment. The results showed that the coactivation technique, which combines solar radiation and air temperature triggers, proved to be the most efficient strategy to improve the performance of the adaptive façade. This strategy minimised heat gain, lowered indoor temperatures, reduced glare, and enhanced daylight comfort, resulting in notable energy savings through reduced cooling consumption. The study concluded that the utilisation of SMP actuators with fine-tuning activation parameters significantly optimised adaptive façade performance, promoting functionality, efficiency, and sustainability in buildings.

Keywords: adaptive facade; shape memory polymer (SMP); actuator; thermoresponsive; building perfromance; simulation

1. Introduction

High-rise apartments are rapidly being built worldwide due to population growth, urbanisation, and lifestyle preferences. As a result, the development of vertical living spaces in dense urban areas, such as the city of Jeddah, has increased dramatically [1]. However, these apartments face several challenges in sweltering hot climates, including high cooling consumption [2] and thermal and visual discomfort [3,4]. Light construction and completely transparent facades are identified as the primary characteristics of high-rise apartments [5] that are not adapted to the sweltering climate, as the gain of solar heat through glazed facades would have caused the occupants to experience significant thermal discomfort and required a considerable amount of cooling energy, accounting for more than 70% of total electricity usage in the Saudi country [6]. In 2021, the Saudi Arabian Ministry of Housing established an energy efficiency code, Mostadam [7], in accordance with Vision 2030 [8] to reduce energy use and carbon emissions targets. However, Mostadam mainly emphasises technical efficiency solutions, such as advanced HVAC systems and lighting, for new projects, with less focus on encouraging property owners to upgrade existing buildings, unlike schemes such as Singapore's Green Mark Incentive Scheme [9]. Furthermore, the code does not promote innovative and sustainable retrofitting solutions or technologies.

Traditional solutions such as fixed shading and insulation help mitigate heat transfer in buildings, but their inability to adapt to environmental changes limits their efficacy, as they provide constant shading, regardless of the fluctuation of outdoor conditions [10]. Instead, shading devices should adapt to daily or seasonal boundary conditions for the future sustainability of buildings. Therefore, an adaptive facade is a building envelope that can dynamically respond and adapt to changing environmental conditions, optimising energy efficiency and overall performance [11]. Using various technologies and intelligent materials, designers create these systems to adapt to changing climate parameters, such as solar radiation, wind speed, and temperature, by adjusting their configurations [12]. Moreover, adaptive facades align with the goal of near-zero energy buildings (nZEBs) of the European Union (EU) by significantly reducing energy consumption and CO2 emissions, thus improving the quality of the internal environment [13], [14]. Numerous studies have extensively examined the potential advantages of adaptive facade systems in terms of improving energy efficiency [15], improving internal comfort conditions, and minimising environmental effects [16], including different types such as shading devices, switchable windows, louvres, and other similar features [17].

The motion of the adaptive system can be operated by human intervention [18] through (manual or interfaces) or automatically [19] through sensors or actuators by integrating intelligent materials (eg SMP, SMA, PCM) [20–22]. Smart material-based actuator shading devices offer the advantages of advanced technologies that function without external sensors or monitor units using the natural response of materials to environmental stimuli [23]. Elements of a building, such as an adaptable envelope, adaptive shading devices, and self-actuating structures, may all benefit from integrating intelligent material actuators because they significantly improve structure flexibility, indoor comfort, energy efficiency, and cost-effectiveness [24].

This study suggests the incorporation of an SMP as an actuator function, allowing the adaptive shading system to switch transitions between open and closed positions, based on previous research on thermoresponsive intelligent materials [20,25,26]. Shape-memory polymer (SMP) actuators are chosen for architectural use over other thermoresponsive materials due to their unique reaction temperatures, recovery of shape, flexible form options, various manufacturing processes, and shape-memory effects [27]. The behaviour mechanism of SMPs allows them to be "programmed" to retain their original shape, undergo significant deformation, and return to their initial form when exposed to specific stimuli such as temperature and solar radiation. The memory of SMPs plays a crucial role in their operation, which is determined by the transition temperature Tg. To achieve this memory effect, a double SMP layer is used with two different glass transition temperatures, Tg1 and Tg2, is used [28]. Above Tg, the SMPs exhibit a soft state, while below Tg, they become rigid.

Previous applications of SMPs as actuators have shown promise, although their use in the architectural field is still in the early stages of design, research, and development. In particular, Steven Beites [29] presented a prototype of an SMP joint, demonstrating the viability of these applications as actuator mechanisms for opening and closing. Similarly, J. Yoon [20] created a hinge prototype that uses thermal stimuli for activation. Therefore, this previous research has demonstrated the possibility and potential of adding SMP actuators as operational in structural systems. However, further research is required to optimise the design and operation of these systems, such as discovering optimal thermal activation, performance evaluation, material testing, operational efficacy, and an adaptable facade system under varying climate conditions. The early design phase investigates the performance of adaptable facades and their thermal activation parameters. The study claims that changing activation parameters can improve energy efficiency and thermal and visual comfort in a hot climate.

2. Adaptive Shading Based on SMP: Principles and Design

Implementing Shape Memory Polymer (SMP) as an actuator in adaptive shading systems allows dynamical management of the thermal response of the building, adjusting peak load times based on climatic variables, and modulating seasonal energy needs. The activation parameters of the SMP material determine how the adaptive shading system works to achieve the desired building performance. The open/closed switching mechanism of an adaptive façade-based SMP is responsive to

Preprints (www.preprints.org) | NOT PEER-REVIEWED | Posted: 14 July 2023 doi:10.20944/preprints202307.0931.v1

changes in external conditions. Therefore, the selection of appropriate stimulus parameters is essential to ensure that the adaptive facade system operates efficiently and effectively in different weather conditions [30] and is necessary to meet the needs of the building and its residents [31]. Numerous investigations have explored various climatic variables for the activation of the adaptive system and have evaluated its effectiveness based on the goal of building performance and the specific location and climate zone of the building [32], including solar radiation [33–35], air temperature [20,36], humidity [36]. Typically, researchers have implemented controls for the adaptive shading system that exceed specific thresholds, using solar radiation control to maintain comfort. However, each study had distinct objectives and climates; therefore, there is no agreement on the efficacy of the activation parameter.

Therefore, this study investigates the ideal activation parameters for the adaptive facade performance based on SMP in a hot environment, considering variables such as air temperature, solar radiation, or a combination of the two. The operation of the adaptive switching mechanism is dictated by the SMP strip, which is thermally sensitive. The sun's heat is a thermal trigger for the SMP strip, allowing it to bend and adjust the shading system.

As shown in Figure 1, the adaptive façade shading module comprises triangular polycarbonate sheets glued to an SMP strip that acts as an actuator. Sun heat causes the SMP strip to bend, shutting off the shading sheets. When the temperature drops, the strip cools and returns to its original position, closing the shade. The design and functioning of this adaptive shading system represent a well-synchronised dynamic between building performance and environmental conditions.

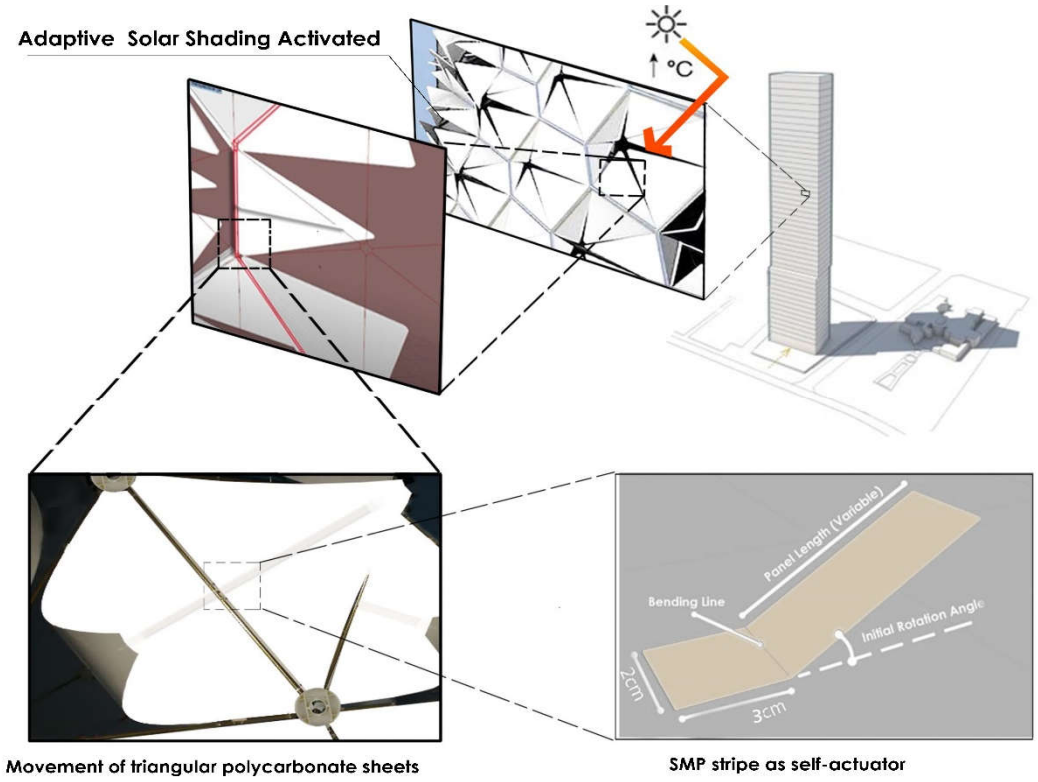

Figure 1. SMP actuator-based adaptive solar shading system.

3. Method

3.1. Thermal Activation

In hot climates, determining the exact temperature or solar radiation threshold at which the shade system starts to operate is critical to balance occupant comfort and energy savings. Therefore, the study comprehensively analyses international standards and guidelines to recommend indoor thermal comfort. Measures, such as ASHRAE standard 55, ISO 7730, and EN 15251, provide

 doi:10.20944/preprints202307.0931.v1

guidelines and metrics for indoor thermal comfort. In the UK, the Chartered Institute of Building Services Engineers (CIBSE) has created meteorological data and static overheating criteria for this reason [37]. The simulation software assesses the requirements by evaluating the thermal performance of the building and determining the hours of overheating based on an interior temperature threshold. The threshold is typically set by the static criteria of the CIBSE to classify a building as overheating if the internal temperature exceeds 25 °C for non-residential buildings and 28 °C for apartments for more than 1% of the hours occupied. The Passivhaus standard [38] establishes a threshold of no more than 10% of occupied hours per year with temperatures above 25 ° C for living areas and 30 °C for other areas, such as corridors.

In Saudi Arabia, Mostadam [39] provides the standard for thermal comfort. The standard is based on the PMV/PPD model, which is adapted from the international standard ASHRAE 55 and ISO 7730. The satisfied people of Jeddah demonstrated that the comfort limits of the PMV ranged between 20.3 ° C and 26.7 °C, ensuring a comfort zone when the PMV is -0.5 to +0.5, and the PPD is less than 10%. However, there is some evidence that adopting these international standards in hot climates can result in summer overcooling, which wastes energy and can cause discomfort for building occupants. Furthermore, recent research by Nuaimi [40] showed that the international standards of PMV are in hot regions (such as the Global South) compared to field data from cities in India, the Philippines, and Thailand, causing 49% more discomfort due to overcooling than ideal interior temperatures. Another study by Elnaklah et al. [41] found that the current international criteria for PMV thermal comfort do not predict thermal experience for 94% of the occupants, as shown by a meta-analysis of four cities in the Middle East (Jeddah, Amman, Dubai, Doha) with 39% discomfort due to overcooling in summer.

An alternative approach to determining interior comfort is provided by the American Society of Heating, Refrigerating, and Air Conditioning Engineers (ASHRAE-55) [42]. This technique takes advantage of the adaptive thermal comfort model [42], which claims that the interior temperature threshold is influenced by the mean ambient temperature of the local climate, as well as the preferences of the occupants. Integrating the adaptive thermal comfort method into this investigation provides valuable information on temperature thresholds that align with the prevailing climatic conditions. Furthermore, the application of the adaptive thermal comfort model becomes vital in determining the appropriate indoor temperature range that ensures the comfort of residents while maintaining energy efficiency in hot and humid climates like Jeddah, where outdoor temperatures can soar to 45 °C. Researchers and organisations have proposed several approaches to establish acceptable indoor temperature ranges based on outdoor conditions. Among these approaches, the widely used adaptive model by Nicol and Humphreys [42] integrates the theory of adaptive comfort and considers the impact of outdoor temperature and humidity on indoor comfort. Another frequently used model is the adaptive Szokolay model [43], which predicts acceptable indoor temperatures in hot and humid climates. Although both models provide valuable information on adaptive thermal comfort, the Nicol and Humphreys models offer a more comprehensive approach, accounting for a wider range of factors that influence thermal comfort. The equations are as follows: (1) Nicol and Humphreys, (2) Szokolay:

$$Tc = 13.5 + 0.54\ To \quad (1)$$

$$Tc = 17.6 + 0.31\ To \quad (2)$$

where: To is the monthly mean of the outdoor air temperature

To assess weather in Jeddah, Climate Consultant 6 software was used with weather files (EPW files) covering 15 years (2007-2021). The software extracted data on average air temperature and relative humidity, as depicted in Figure 2, illustrating annual averages. In particular, July and August emerged as the hottest months, while January and February were the coldest.

Preprints (www.preprints.org) | NOT PEER-REVIEWED | Posted: 14 July 2023 doi:10.20944/preprints202307.0931.v1

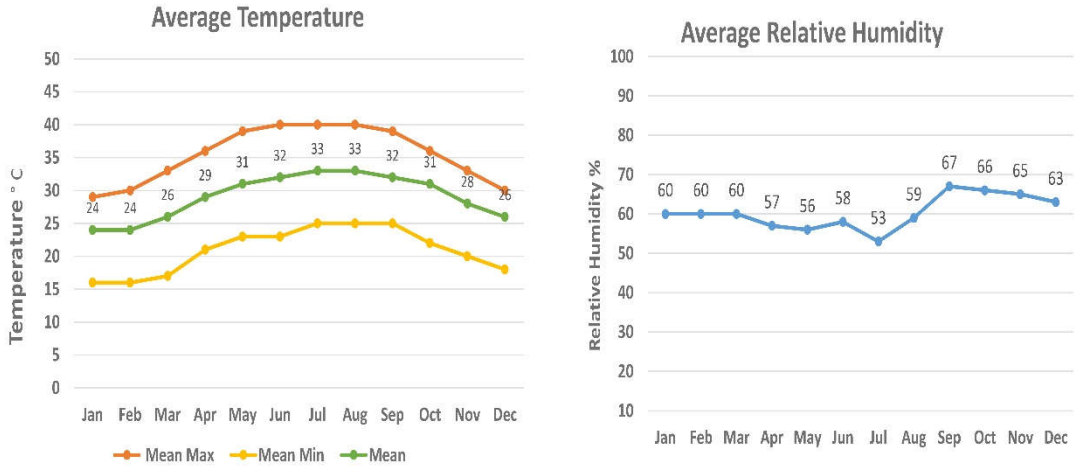

Figure 2. Average air temperature and relative humidity in Jeddah.

As shown in Table 1, the results of the Szokolay, Nicol and Humphreys models based on average outdoor temperatures, which are calculated year-round, offer an alternate way of determining the appropriate range of indoor comfort temperatures in hot climates like Jeddah city. The average outdoor temperature in July and August was 33°C. The Nicol and Humphreys equation yields a comfort temperature of 31.3 °C and a comfort range of 29.3 to 33.3 °C (+/- 2). The second Szokolay equation-based examination found a comfort temperature of 28 °C and a comfort range of 25.5 to 30.5 °C (+/- 2.5).

Table 1. The adaptive thermal comfort limit in Jeddah with the Nicol and Szokolay formulas.

Comfort limit Nicol and Humphreys (range -/+ 2)°C					Comfort limit Szokolay (range -/+ 2.5) °C				
Months	**Outdoor Avg. Temp**	**Thermal Comfort**	**Lower**	**Upper**	**Months**	**Outdoor Avg. Temp**	**Thermal Comfort**	**Lower**	**Upper**
Jan	24	26.4	24.4	28.4	**Jan**	24	25.0	22.5	27.5
Feb	25	27	25	29	**Feb**	25	25.3	22.8	27.8
Mar	26	27.5	25.5	29.5	**Mar**	26	25.6	23.1	28.1
Apr	29	29.1	27.1	31.1	**Apr**	29	26.5	24	29
May	31	30.2	28.2	32.2	**May**	31	27.2	24.7	29.7
Jun	32	31	29	33	**Jun**	32	27.5	25	30
July	33	31.3	29.3	33.3	**July**	33	28	25.5	30.5
Aug	33	31.3	29.3	33.3	**Aug**	33	28	25.5	30.5
Sep	32	31	29	33	**Sep**	32	27.5	25	30
Oct	30	29.7	27.7	31.7	**Oct**	30	26.9	24.4	29.4
Nov	28	28.6	26.6	30.6	**Nov**	28	26.2	23.7	28.7
Dec	25	27	25	29	**Dec**	25	25.3	22.8	27.8

Based on the Nicol model, this investigation established the 33 °C air temperature threshold as the activation point for the air temperature-activated adaptive shading system. This determination was made considering the data obtained in August, the hottest month. Figure 3 shows Jeddah's monthly mean adaptive thermal comfort based on the outside temperature.

Preprints (www.preprints.org) | NOT PEER-REVIEWED | Posted: 14 July 2023 doi:10.20944/preprints202307.0931.v1

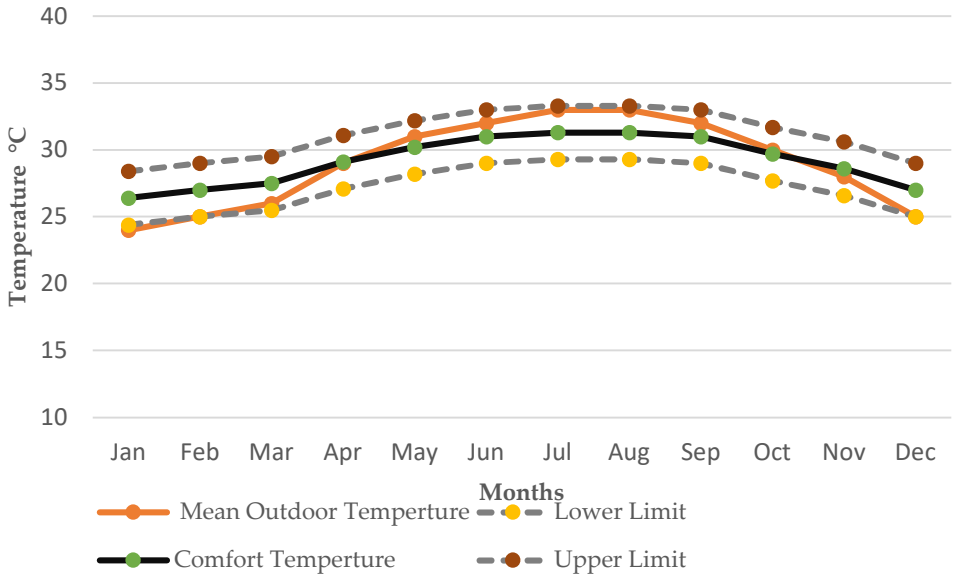

Figure 3. The monthly adaptive thermal comfort limit in Jeddah, based on the Nicol formula.

The adaptive Nicol model also allows for a wider range of acceptable temperature variations, which may be particularly relevant in hot-humid climates such as Jeddah, where occupants prefer a slightly warmer indoor temperature. Furthermore, a study by Nicol and Humphreys found that people in hot-humid regions adapt to high temperatures, such as 33 ° C in Pakistan and even 34 °C in Sri Lanka when the airspeed increases to 0.6m/s.

However, accurately identifying the solar radiation threshold for activating the shading system is essential to optimise its operation, effectively balancing heat gain control and maximising the daylighting performance. Using IES-VE, the average direct sun radiation level in Jeddah was calculated to be 275 W/m2, applied to the system activation point. This approach involved estimating the direct solar radiation threshold, as shown in Figure 4, considering the average value measured in August.

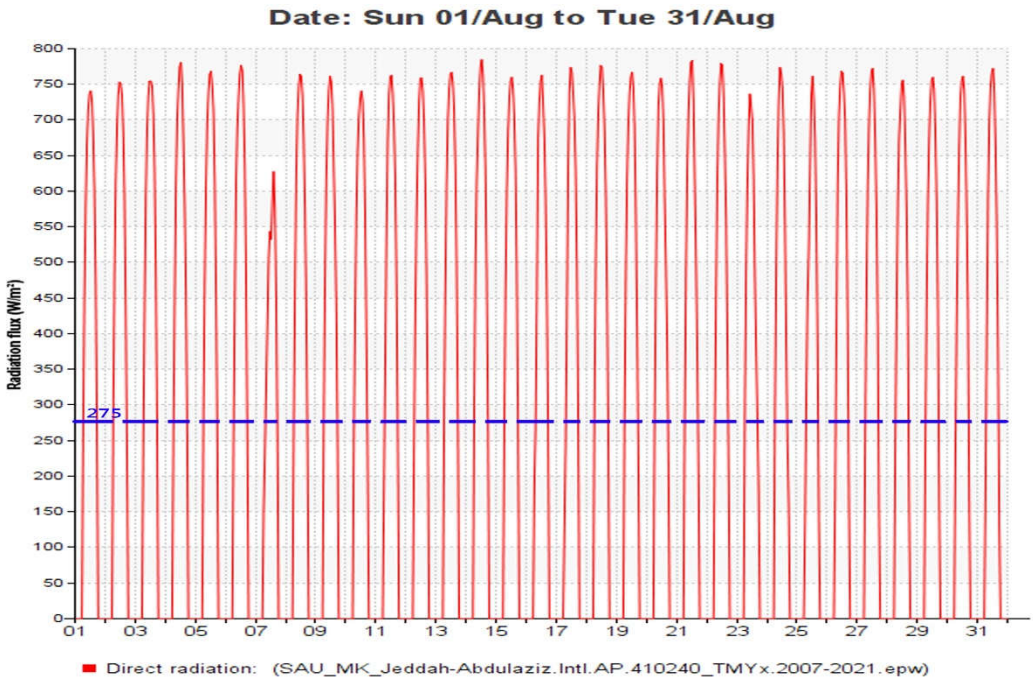

Figure 4. August's average levels of direct solar radiation in Jeddah.

 doi:10.20944/preprints202307.0931.v1

However, daylight performance is often given less priority in Saudi Arabia, mainly due to cultural and practical considerations. One reason for the lower emphasis on daylighting is the relatively small proportion of lighting energy consumption compared to cooling and overall energy use in buildings. According to a report by the Saudi Energy Efficiency Centre, lighting represents only approximately 14% of total energy consumption in commercial and residential buildings in the country (Saudi Energy Efficiency Centre, 2021) [44] and is much less than 70% of the energy consumed by cooling and maintaining thermal comfort in buildings in the hot and arid climate of Saudi Arabia. Another factor contributing to the lower importance of daylighting performance in Saudi Arabia is the widespread use of artificial lighting in households due to cultural and privacy concerns [45]. In many Saudi homes, it is customary to keep curtains and blinds closed to maintain privacy and avoid exposure to the outside world. Therefore, artificial lighting often illuminates indoor spaces, even during the day.

When evaluating daylight performance in Saudi Arabian buildings, the Mostadam code [7] prioritises specific requirements over the daylight factor (DF) as a metric. For instance, it emphasises achieving a minimum average daylight illuminance of 200 lux for residential spaces, with at least 50% of the required illuminance coming from daylight. On the contrary, the EN 17037 European Daylight Standard [46] prescribes a minimum DF of 2% for visual comfort, equivalent to a minimum level of illumination of 300 lux under conditions of clear sky. Therefore, considering the EN 17037 European Daylight Standard is a valuable metric for assessing daylight performance in this study.

3.2. Simulation tool and weather data

To investigate the impact of the adaptive facade system on the energy and thermal performance of buildings, the selection of appropriate Building Performance Simulation (BPS) software is crucial. Various options are available on the market [47](eg EnergyPlus, ESP-r, ICE, and IES-VE) to model and simulate the thermal performance and energy of buildings under different conditions, such as changes in climate, occupancy patterns, and building systems. For this investigation, IES- VE software is used due to its ability to simulate dynamically and assess the thermal performance of the adaptive façade and its impact on indoor conditions and energy in response to factors based on operational profile, such as occupancy patterns and external environment control, such as temperature and solar radiation. Furthermore, the study uses the IES-VE programme and(EPW) files to extract precise weather data for Jeddah, covering 15 years from 2007 to 2021. Using long-term historical weather data is a common practice to establish a baseline and evaluate building performance under realistic and documented climatic conditions that have occurred in the past.

Located on the coast of the Red Sea in western Saudi Arabia, Jeddah is located at coordinates (21°68′N and 39°16′E). Jeddah falls under the Kappen Climate Classification of BWH, which signifies an arid desert-hot climate. However, due to its proximity to the Red Sea, Jeddah experiences a unique hot and humid climate [48]. Based on the analysis conducted using the IES software, Jeddah experienced its highest temperatures in July and August, reaching a peak of 49 °C on August 24. In contrast, the coldest months are January and February, with temperatures dropping to a low of 15 °C on January 9. Figure 5 illustrates Jeddah's sun path and angle, utilising the sun cast feature in the IES-VE software, revealing that the sun's path is orientated southward during the winter and moves towards the middle and northward during the summer.

Preprints (www.preprints.org) | NOT PEER-REVIEWED | Posted: 14 July 2023 doi:10.20944/preprints202307.0931.v1

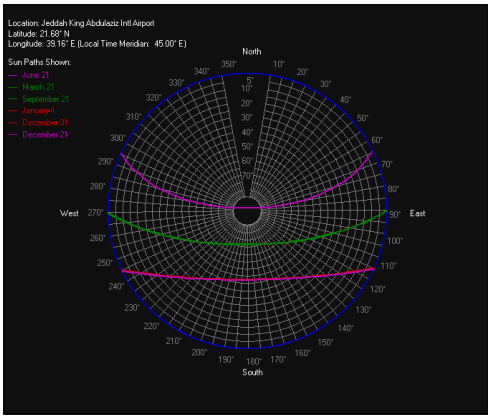

Figure 5. Jeddah Sun Path Diagram Generated by IES -VE Simulation.

3.3. Apartment Conditions: as a case study

This study examines a high-rise apartment in the city of Jeddah. The building has a significant amount of glazing on its facade and a low thermal mass, representing the typical architectural style observed in the area. With a height of 205 metres, 48 floors, and a total of 78 residential apartments, this skyscraper was constructed in 2017. Each floor comprises two identical apartments, each with an average area of 420 square metres, and the building offers apartments with three different orientations. Figure 6 shows the layout of the apartment on the 25th floor, which serves as the benchmark for evaluation and validation. The apartment has three different facade orientations: South, East and West. In particular, the living room (84m²) and bedroom (20m²) are located toward the west and south facades. As a result of the intense penetration of solar heat through these orientations, overheating and potential discomfort for residents are expected to increase.

Figure 6. The layout and viewpoint of a skyscraper residence in Jeddah.

The study conducted detailed modelling of the bedroom and living room, including its details, layout, building materials, interior finishes, lighting and occupancy. These data were collected through site observations, resident interviews, and project management records. The thermal properties and construction materials of the benchmark apartment are summarised in Table 2. In addition, internal heat gain data was obtained from the ASHRAE Guide [49] to ensure precision in the simulation. Lighting, appliances and people(parents with three children) according to an operating profile all contribute to the modelling of internal heat gain, as shown in Table 3.

Preprints (www.preprints.org) | NOT PEER-REVIEWED | Posted: 14 July 2023 doi:10.20944/preprints202307.0931.v1

Table 2. External thermal and structural criteria of the apartment.

Thermal Characteristics of Apartment Conditions			
Surface	**Variables**	**Values**	**Materials Description**
Wall	U-value	1.46 W/m²K	Layers from outside to inside:
	Thickness	230 mm	1- Sandstone 100mm
	Solar absorptance	0.9	2-Cavity 100mm
	Emissivity	0.7	3- 10mm cement-bonded 4-Gypsum board 20mm
Windows	U-value	2.68W/m²k	
	Thickness	24mm	Double-insulating glass:
	Emissivity	0.83	1- Outer 6mm
	Transmittance	0.71	2-Cavity 12mm
	SC Shading Coefficient	0.45	3-Inner 6mm
	Glazing Ratio WWR	80%	
Floor Celling	U-value	3.12 W/m²K	1- Reinforced Concrete100mm
	Thickness	200mm	2-Screed 50mm
	Solar absorptance	0.55	3- Marble 50mm
	Emissivity	0.9	
Internal partition	U-value	1.52W/m²K	1- 25mm Plasterboard
	Thickness	100 mm	2-Cavity 50mm
	Solar absorptance	0.55	3- 25mm Plasterboard
	Emissivity	0.9	

Table 3. The internal gain and operating time of the equipment.

Internal Heat Gain					
Space	**Type**	**Gain**	**Operating times**		
			11 pm-7 am	**7 am-3 pm**	**3 pm-11 pm**
Living room	5 people	75 w/person	off	off	on
	appliances	550 w	off	off	on
	lighting	252 w	off	off	on
Bedroom	2 people	50 w/person	off	on	on
	appliances	50 W	off	on	on
	lighting	60 W	off	on	on

3.4. Configuration and operating schedule

The adaptive façade shading system incorporates an innovative SMP material as an actuator, allowing it to dynamically adjust to outdoor variables such as solar radiation and air temperature. The open and closed mechanism of the switch system was performed using the external louvre feature and the operational profile settings with control thresholds in the IES-VE software to calculate an operating schedule. The operational profile function in IES-VE software governs this process, while a daily thermal template manager defines the system's state control based on a thermal activation threshold. Three distinct activations guide the behaviour of the system: operation based on the temperature of the outside air temperature (≥ 33 °C), operation based on direct solar radiation, therefore, the coding reads (≥ 275 W/m²), and a combination of both factors; thus, the code is written (to >= 33) I (idn >= 275). Figure 7 shows these conditions and their corresponding formulas.

Preprints (www.preprints.org) | NOT PEER-REVIEWED | Posted: 14 July 2023 doi:10.20944/preprints202307.0931.v1

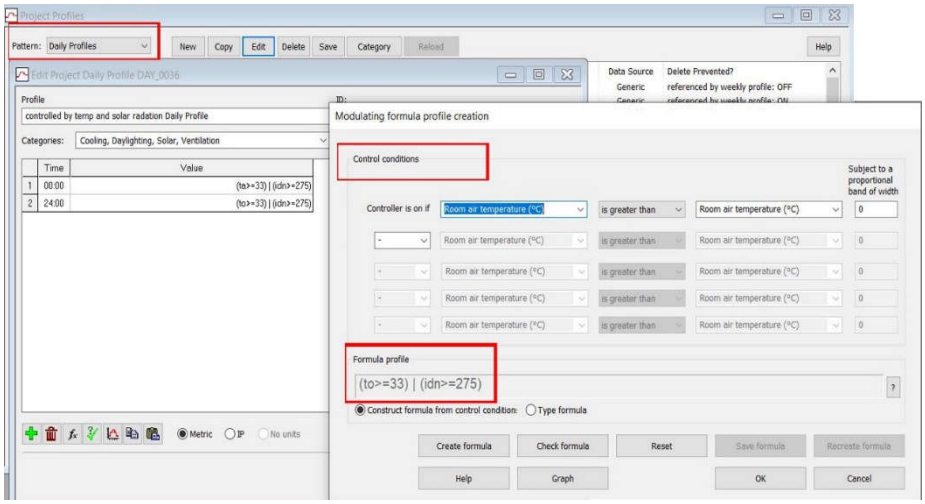

Figure 7. Process of setting IES by operational profile for the system control.

In the final step of the setting process, Figure 8 shows the selection of exterior shading types for the bedroom and living room using the project construction tool. Louvres respond to climatic activation factors determined by control settings, allowing them to open or close accordingly. For example, if the outdoor temperature exceeds 33 °C, the louvre device will be lowered and set to 0, providing maximum shading. In contrast, when the outdoor temperature falls below 33 °C, the louvre shading will increase and be set to 1, allowing more natural light and ventilation.

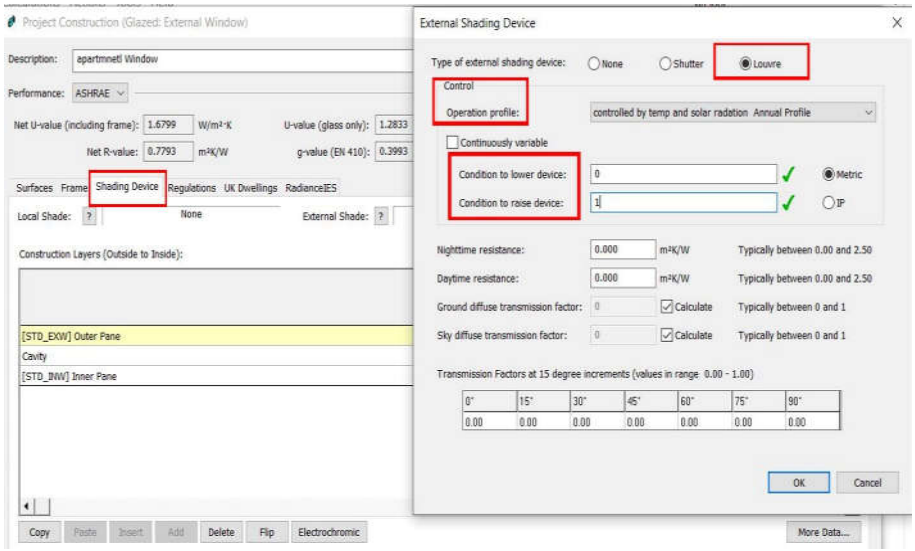

Figure 8. The final setting step uses a louvre shading with activation conditions.

The following schedule outlines the operation of the shading system based on the settings and conditions described above. Figure 9 illustrates the dynamic behaviour of the shading system's operation on the west and south facades, estimated for August 24. Daily fluctuations influence the switching behaviour of the adaptive facade shading system in climatic conditions and activation thresholds.

On the south facade, the operating time shows that the adaptive shading will be closed for 8 hours between 8 am and 16:00 and will remain open for the rest of the day if the combination scenario is implemented. Alternatively, if the solar radiation activation scenario is selected, the system will be closed for 3 hours between 11:00 a.m. and 14:00, but will remain open for the rest of the day. Lastly, the air temperature scenario will be closed for the entire day, except for 7 hours between 1 am and 8:00 am to be open.

Preprints (www.preprints.org) | NOT PEER-REVIEWED | Posted: 14 July 2023 doi:10.20944/preprints202307.0931.v1

However, the west façade timetable shows the exact period of operation by 8 hours in the combo scenario, while the closure time changed between 9:00 am and 17:00. Furthermore, the air temperature-driven activation timeframe for adaptive shading aligns with that of the southern facade. However, there is a slight difference in the solar radiation scenario; the closure time is afternoon from 13:00 to 17:00, an hour longer than the southern facade. Figure 10 shows the closure period of the adaptive shading system under different control situations.

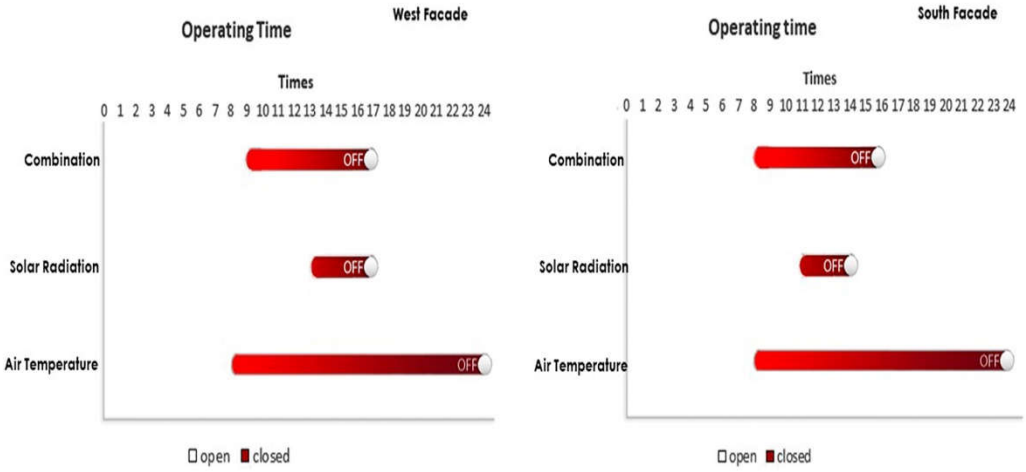

Figure 9. The timetable of system operation under multiple activations - August 24.

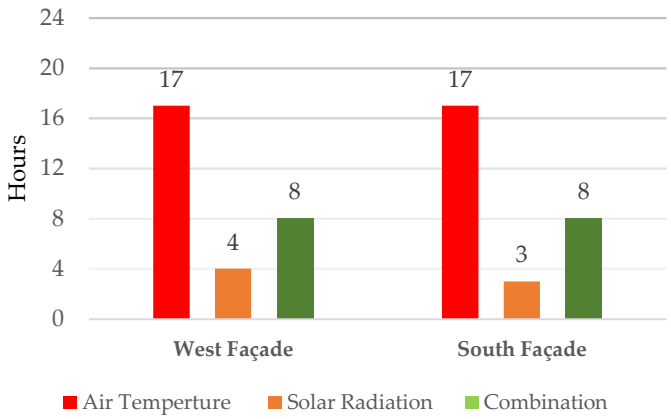

Figure 10. Total operational hours of adaptive façade under multiple activations - August 24.

4. Results

The results were validated by comparing the thermal performance of the adaptive facade with the bare glazing facade on a summer day, focussing on thermal comfort, energy efficiency, and visual comfort to evaluate the effectiveness of activation parameters. The effectiveness of various activation parameters in regulating solar radiation, mitigating solar heat gain, optimising daylighting, reducing glare, and improving indoor temperature and occupant comfort are evaluated. The evaluation was carried out on August 24, considering three different activation scenarios: air temperature, solar radiation, and a combination. The living room and bedroom of the apartment were evaluated using the IES-VE simulation tool with ApacheSim and Sun-Cast's model.

The simulations calculated the room's temperature and thermal comfort under different climate control strategies, with the cooling system turned off to avoid any interference with the overheating assessment. However, to evaluate the overall performance of the building, the cooling system was activated to a set point temperature of 23 °C, recommended by ASHRAE Standard 55 for indoor thermal comfort. The energy consumption and cooling load were analysed to determine the efficiency

Preprints (www.preprints.org) | NOT PEER-REVIEWED | Posted: 14 July 2023 doi:10.20944/preprints202307.0931.v1

of the adaptive shading system. The results of these simulations provide valuable information on the effectiveness of activation parameter strategies in optimising adaptive shading performance, considering the three criteria thermal comfort, visual comfort, and energy efficiency.

4.1. Thermal Comfort Evaluation

4.1.1. Indoor Temperature

In hot climates, building temperature regulation is crucial for occupant comfort. Excess solar gain increases indoor temperature, occupant discomfort, and health risks related to heat. Thus, adaptive shading controls solar gain and interior temperature of the building. This study used the operating temperature to represent the internal temperature since it incorporates the air temperature and the average radiant temperature. The simulation results of the three adaptive facade control scenarios were compared with the reference model of the living room (double-facing south and west) and the bedroom (single-facing south) to determine the effectiveness of the climatic variables control method in optimising adaptive system performance. On August 24 a summer day, the simulations were conducted at (6 a.m., 9 a.m., 12 p.m., 3 p.m., and 6 p.m.) to account for the solar gain influence at different times.

The simulation results demonstrate the effectiveness of adaptive shading activation variables in increasing interior temperatures throughout the day compared to the base-case facade. Figure 11 shows a comparison between the current façade and the adaptive façade controlled by three different scenarios of climate variables in the operative temperature of the living room and bedroom. The results showed that the combination scenario had the most notable improvement in indoor temperatures and reduced overheating in both the living room and the bedroom, followed by the air temperature scenario, while the solar radiation scenario was the worst, showing no change in the living room at any time except a slight improvement in the bedroom in the morning.

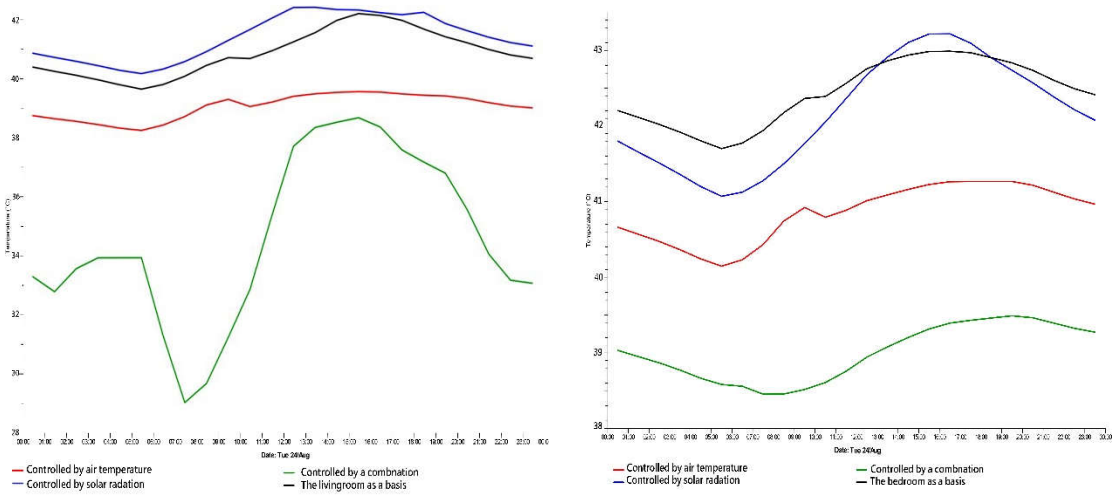

(**a**)Livingroom (**b**)Bedroom

Figure 11. Interior temperature in baseline Vs. Adaptive façade activation parameters - August 24.

Table 4 shows that the combination scenario in the living room on August 24 shows the greatest reduction in the average indoor temperature, decreasing from 40.5°C to 35,3 ° C with 5.2°C differences. The highest reduction of 20% at 9 am in indoor temperatures dropped from a reference of 40.2°C to 31.9°C, an 8.3°C decline. Furthermore, the living room base model showed a maximum temperature of 41.5 °C at 3 p.m., while the combination scenario improved the temperature to 38.6°C, a difference of around 2.9 °C, approximately 7%. Similarly, the combination scenario was the most effective in the bedroom, with the most significant decrease of 10% at 12 p.m. from the baseline temperature of 42.7°C to 38.5°C, leading to a fall of around 4.2°C. Furthermore, the bedroom base model indicated a maximum temperature of 43 °C at 3 p.m., while the combination scenario reduced the temperature by approximately 3.9 ° C or 9%.

Preprints (www.preprints.org) | NOT PEER-REVIEWED | Posted: 14 July 2023 doi:10.20944/preprints202307.0931.v1

Table 4. Interior temperature in the baseline Vs. Adaptive façade activation parameters - August 24.

Type of Space	Living room °C					Bedroom°C				
Time	6 a.m	9 a.m	12 p.m	3 p.m	6 p.m	6 a.m	9 a.m	12 p.m	3 p.m	6 p.m
The basic case	39.5	40.2	40.7	41.5	41.3	41.7	42.3	42.7	43	42.9
The Air Temperture	38.4	39.1	39.2	39.4	39.3	40.2	40.8	40.9	41.2	41.3
The Solar Radiation	40	40.5	41.3	41.7	41.5	41.1	41.6	42.5	43.1	43
The Combination	33.7	31.9	36.9	38.6	37.6	38.6	38.4	38.5	39.1	39.7

Furthermore, the activation parameters were evaluated under different circumstances throughout the year, including the hottest and coldest months, to determine the effective one. Table 5 illustrates the annual mean difference in indoor air temperature between the bare and adaptive facades in the activation parameter scenarios. The results showed that the combination scenario offers the greatest improvement during summer and winter. However, the variables of air temperature and solar radiation control an adaptable facade in various ways. The solar radiation scenario is more effective in winter than the air temperature scenario in summer. Thus, the annual results showed that the combination variable most effectively lowered the interior temperature, with the second being followed by solar radiation control.

The annual results showed that the adaptive facade combination control reduces the average internal temperature by 6 ° C or 16% and 7.1 ° C or 18% in the living room and bedroom, respectively, from 37.4 to 31.4 ° C and 39.6 to 32.5 ° C. Furthermore, solar radiation is a second ideal scenario, reducing the mean temperature by 2.2 ° C and 3.1 ° C in the living room and bedroom, respectively, while the worst-case scenario involves air temperature control, increasing the average temperature by approximately 0.5 °C.

Table 5. Interior temperatures in the baseline Vs. Adaptive façade activation parameters – Yearly.

Type of Space	Living room	Bedroom
Period	Annual	Annual
The basic case	37.4	39.6
The Air Temperature	38.1	40.2
The Solar Radiation	35.2	36.5
The Combination	31.4	32.5

4.1.2. Discomfort Hours

In this study, the adaptive comfort method evaluates the hours of overheating and discomfort that consider the dynamic interaction between the occupant and the local climate and tries to give a more flexible approach to thermal comfort. As stated previously, comfort levels range between 33.3°C and 29.3°C based mean outside temperature of August using the Nicol TC equation. The operative temperature is a helpful indicator for assessing the comfort level of a building's interior since it considers both the air temperature and the mean radiant temperature. Comparison of adaptive facade activation options in the living room and bedroom to discover the most effective solution to improve thermal comfort. Figure 12 compares hours above the comfort level for a living room facing the southwest on August 24. The results showed that the adaptive facade controlled by the combination improved thermal comfort at the given times, whereas the adaptive shading controlled by the air temperature scenario and solar radiation failed to achieve the comfort level. Compared to the reference model, where the temperature exceeds the comfort threshold for 24 hours and the discomfort ratio is 100%, the adaptable facade controlled by a combination reached the target comfort level in living rooms in 4 hours between 6 and 10 a.m. Furthermore, the living room temperature was not comfortable at 12 pm, 3 pm and 6 pm, except at 6 am and 9 am, once the outside temperature dropped.

Preprints (www.preprints.org) | NOT PEER-REVIEWED | Posted: 14 July 2023 doi:10.20944/preprints202307.0931.v1

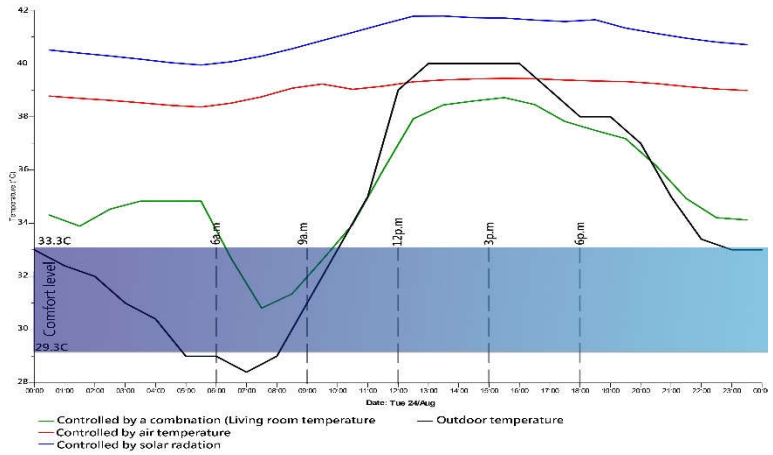

Figure 12. Comparing living room comfort hours under varying activation parameters August 24.

On the contrary, Figure 13 shows that only the adaptable facade controlled by the combined scenario improved thermal comfort in the bedroom facing the south on August 24. Compared to the baseline model, where the temperature exceeds the comfort threshold all day, the adaptable facade controlled by a combination of variables actuated the close position and achieved the target comfort level in the bedroom for 2 hours between 7 a.m. and 9 a.m. Furthermore, the bedroom temperature did not reach a comfortable level at 6 am, 12 pm, 3 pm or 6 pm on July 6, unless at 9 am, when the outside temperature was 31 °C.

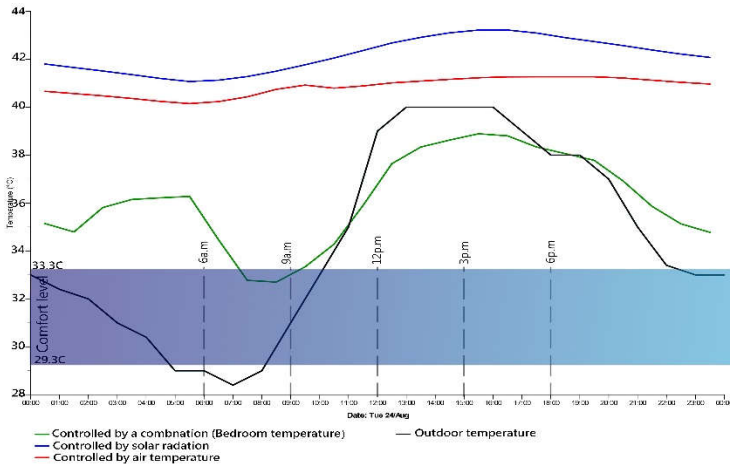

Figure 13. Comparing bedroom comfort hours under varying activation parameters August 24.

Figure 14 shows that the discomfort ratio in the baseline living room was 90% and in the bedroom 97.7% annually. Therefore, using a combined scenario improves the comfort of the living room and bedroom by 50.8% and 44.7 %, respectively. The second scenario is solar radiation, which increases comfort hours by 26% in the living room and by 24.7% in the bedroom. However, the air temperature scenario did not improve comfort hours; it increased discomfort. Figure 15 compares the discomfort hours of the combined scenario with the baseline. Of the 8760 occupation hours, the living room experienced 7870 hours and the bedroom experienced 8595 hours, exceeding the adapted comfort threshold. The adaptive facade through combination control decreases these hours by 3437 and 4644, respectively. The adaptive facade of the combined control improves thermal comfort for 4 661 hours in the living room and 3 551 hours in the bedroom.

Preprints (www.preprints.org) | NOT PEER-REVIEWED | Posted: 14 July 2023 doi:10.20944/preprints202307.0931.v1

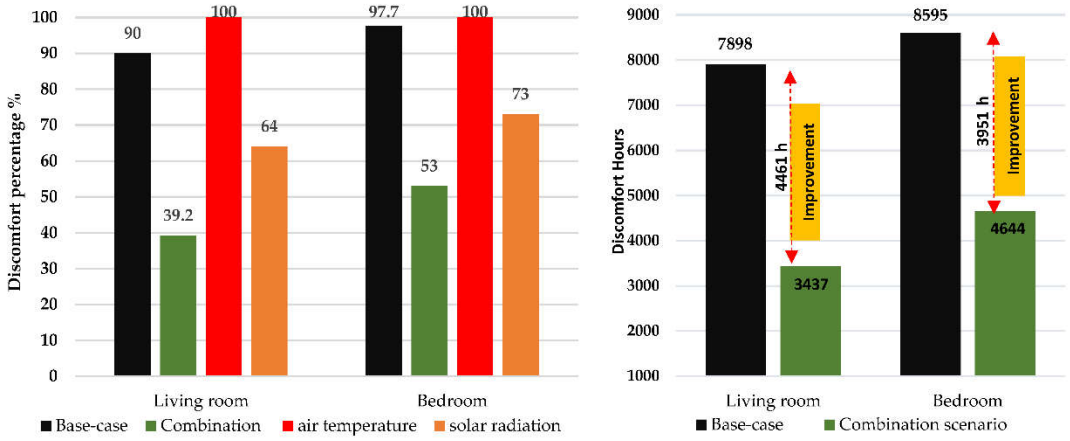

Figure 14. Comparing yearly discomfort ratios in Figure **15**.Comparing the annual improvement hours.

4.2. Visual Comfort Evaluation

4.2.1. Daylighting Performance

Maintaining a balance between optimising natural lighting and preventing heat is challenging when fully closed adaptive facades are activated. Therefore, this study proposes a compromise solution of a 50 cm air cavity between the building and the adaptive system, allowing natural light even when the shading is closed, as shown in Figure 16.

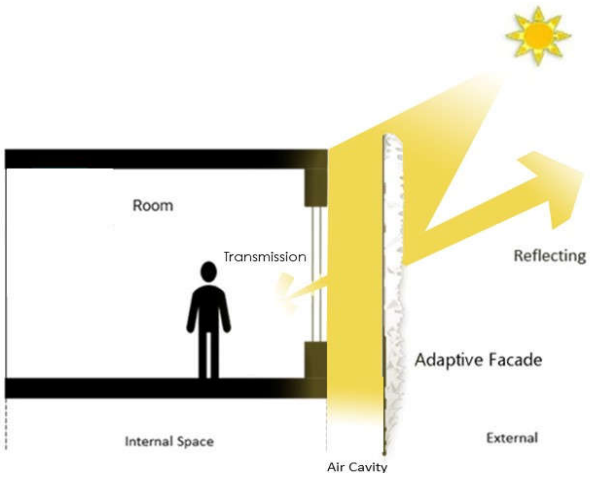

Figure 16. Optimising daylighting in the adaptive system by an air cavity.

In this study, the impact of the adaptive façade was evaluated using the European Daylight Standard, EN 17037 [46], which considers the daylight factor (DF) and measured illuminance levels in lux. For visual comfort, the EN standard prescribes a minimum daylight factor (DF) of 2% and a minimum illuminance level of 300, covering at least 50% of the occupied floor area in a space lux under a clear sky. The dynamic mechanism of the adaptable facade that affects the evaluation of daylighting performance at a given time on August 24 at 3 p.m. was simulated in IES VE using the Radiance IES tool. The results showed that the combination scenario and air temperature scenario were the same, activating the closed position on both the south and west sides, while the solar radiation-activated closed mode only on the west side and unactivated on the south side kept the shading open.

Figure 17 illustrates the significant improvement in daylighting and visual comfort achieved by the adaptive facade compared to the baseline living room activated by air temperature or a combination scenario. The average daylight factor (DF) in the adaptable facade is 2.2%, which meets the target,

Preprints (www.preprints.org) | NOT PEER-REVIEWED | Posted: 14 July 2023 doi:10.20944/preprints202307.0931.v1

while in the baseline facade, the DF is greater than 9.0. This indicates that the adaptive facade provides better daylight conditions and reduces the need for artificial lighting. Furthermore, the adaptive facade ensures that only 54.3% of the living room area experiences a daylight threshold lower than 2 DF, resulting in improved visual comfort throughout the space. Thus, artificial light is required for the living room's rear, with the adaptable façade activated in a closed position on both sides.

Figure 18 shows the impact of solar radiation on the adaptive facade, precisely at 3 p.m., where the south side is opening while the west side is closing. The comparison includes the daylight factor (DF) and the threshold for the baseline and adaptive facades. In this scenario, the adaptive facade exhibits a slight decrease in daylight with an average DF of 8, potentially leading to some discomfort due to glare. However, it is essential to note that no daylight factor thresholds (DF) were observed below 2, indicating that additional artificial lighting is unnecessary.

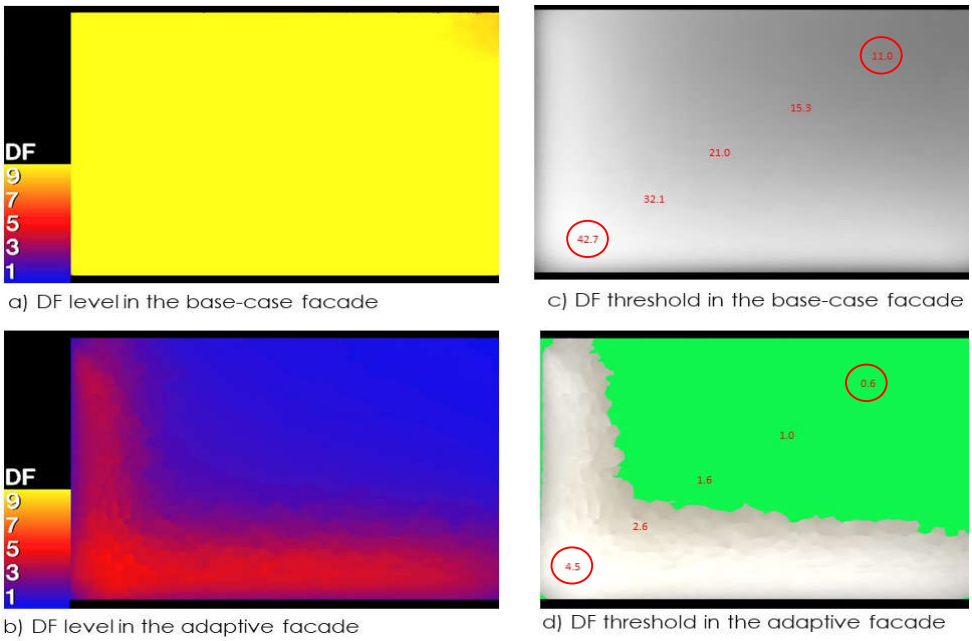

Figure 17. Daylight factors in the baseline Vs. adaptive façade activated by combined temperature.

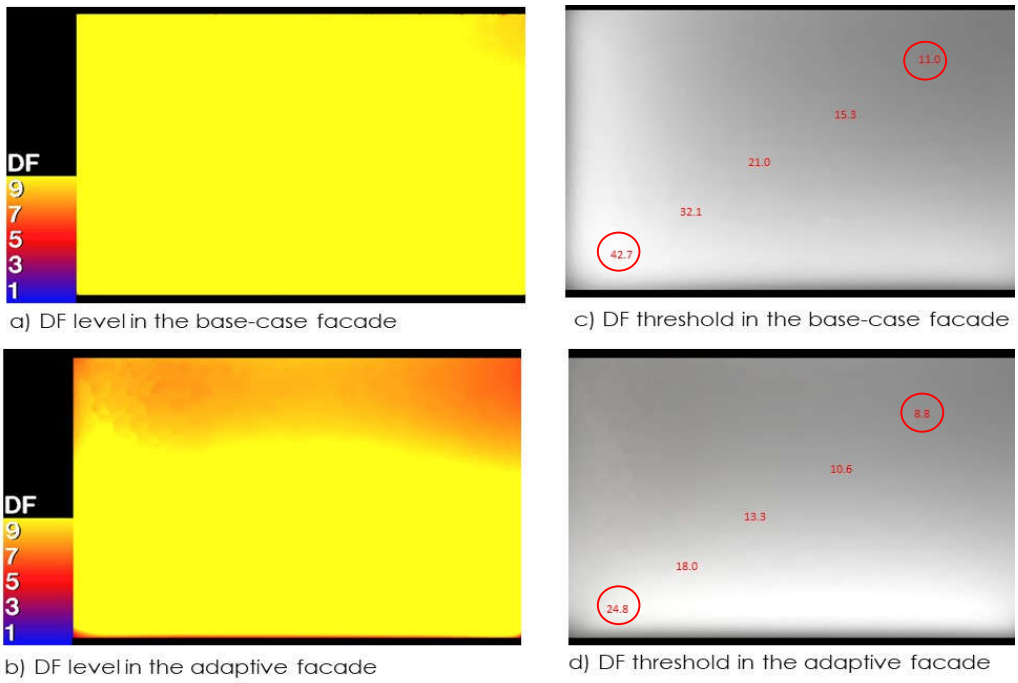

Figure 18. Daylight factors in the baseline Vs. adaptive façade activated by solar radiation.

Preprints (www.preprints.org) | NOT PEER-REVIEWED | Posted: 14 July 2023 doi:10.20944/preprints202307.0931.v1

Figure 19 shows the analysis of the level of illuminance (lux), where the adaptive façade controlled by the air temperature and the combination scenario achieved an average level of illuminance of 323 (lux) in 46.6% of the living room area. Compared to the standard façade, the average illumination was 3200 (lux). In particular, the intensity of illumination achieved by this scenario was 53.4% less than the 300 lux threshold, indicating that the adaptive facade could provide adequate natural illumination and meet the code requirements, but needed artificial lighting.

Figure 20 shows the analysis of the adaptive facade controlled by solar radiation, which achieves an average illuminance level of 2234 (lux) compared to 3200 (lux) for the baseline facade. The analysis did not reveal illuminance levels below 300 (lux), indicating that artificial lighting is unnecessary and can lead to reduced lighting energy usage.

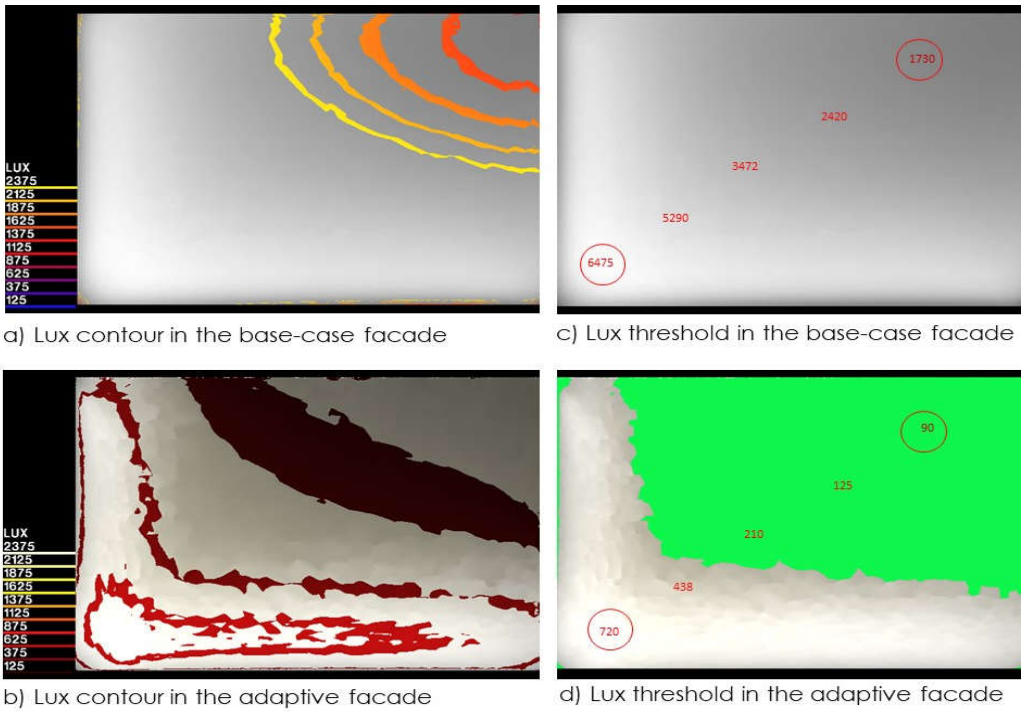

Figure 19. Illuminance levels in the baseline Vs. adaptive façade activated by combined temperature.

Preprints (www.preprints.org) | NOT PEER-REVIEWED | Posted: 14 July 2023 doi:10.20944/preprints202307.0931.v1

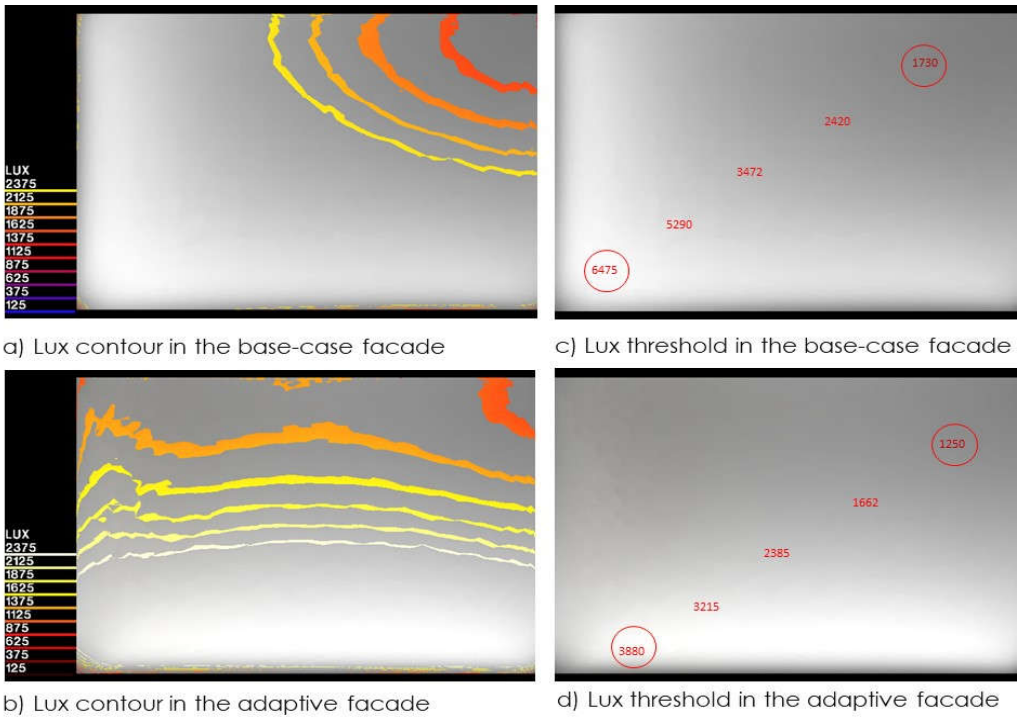

Figure 20. Illuminance levels in the baseline Vs. Adaptive façade activated by solar radiation.

4.2.2. Glare Analysis

Excess brightness can result in glare, which is a significant cause of visual discomfort. The IES-VE simulation evaluates glare using the daylight glare probability (DGP) metric. This metric categorises the percentage of people affected by glare into four categories:

1. Imperceptible; less than 35%
2. Perceptible;between 35%-40%
3. Disturbing;between 40%-45%
4. Intolerable: greater than 45%

Figure 21 illustrates the evaluation carried out in the living room at 3 p.m. on August 24 to determine the level of glare. The results found that the glare level was 89.94 % higher than the 45% threshold, which is considered intolerable and indicates that the glare in the living room was considerably more intense and could cause discomfort.

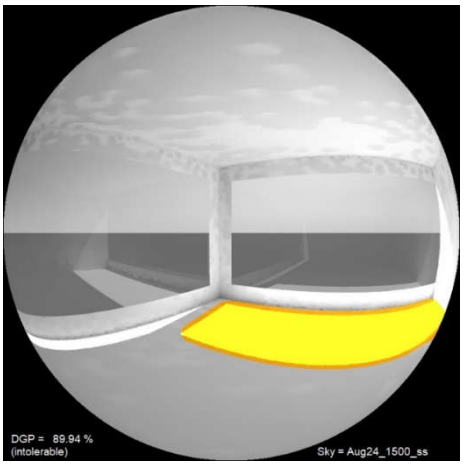

Figure 21. DGP with the baseline façade.

Preprints (www.preprints.org) | NOT PEER-REVIEWED | Posted: 14 July 2023 doi:10.20944/preprints202307.0931.v1

Figure 22 illustrates the installation of the adaptive shading system and its activation in response to the combination scenario or the air temperature scenario. When activated, the system closed both sides of the room, reducing glare by 26.25% but restricting visibility. This reduction is below the imperceptible threshold of 35%, indicating a significant improvement in visual comfort in the living room with the activation of the combined parameters. However, as illustrated in Figure 23, when solar radiation activates the adaptive facade, the shading closes on the west side of the room while remaining open on the south side, allowing visibility, lowering the glare to 36.75% and showing a perceptible threshold between 35 and 40%.

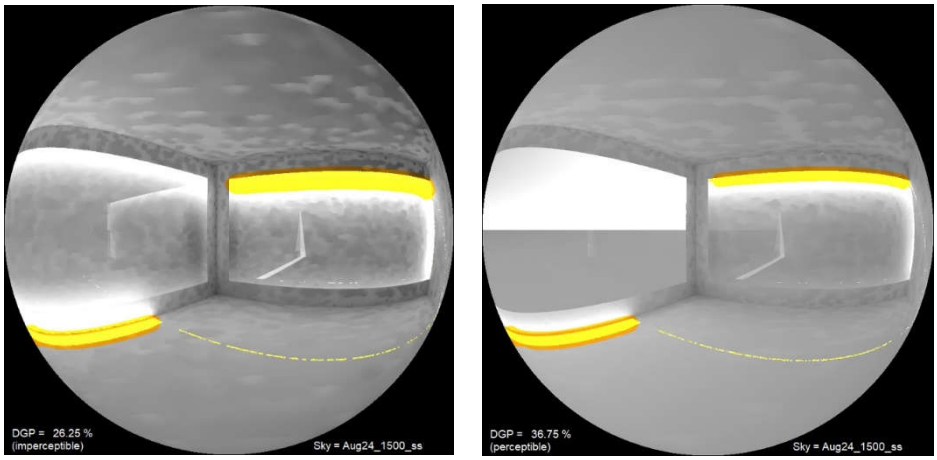

Figure 22. DGP analysis with combined activation **Figure 23**.DGP analysis with solar radiation activation.

4.3. Energy Efficiency Evaluation

4.3.1. Solar Heat Gain

Minimising solar heat absorption is critical for designing energy-efficient buildings in hot climates. Sun heat has the potential to significantly increase heat penetration into a building, leading to discomfort for occupants, increased reliance on air conditioning, higher energy costs, and increased greenhouse gas emissions. Therefore, dynamic shading strategies are applied to effectively track and regulate solar heat absorption in building designs. Figure 24 illustrates the influence of solar radiation on cooling loads in a room with glazed and adaptable facades when the adaptive shading of a building operates in closed positions during the day based on heat activation, preventing and reflecting solar radiation, and improving energy efficiency.

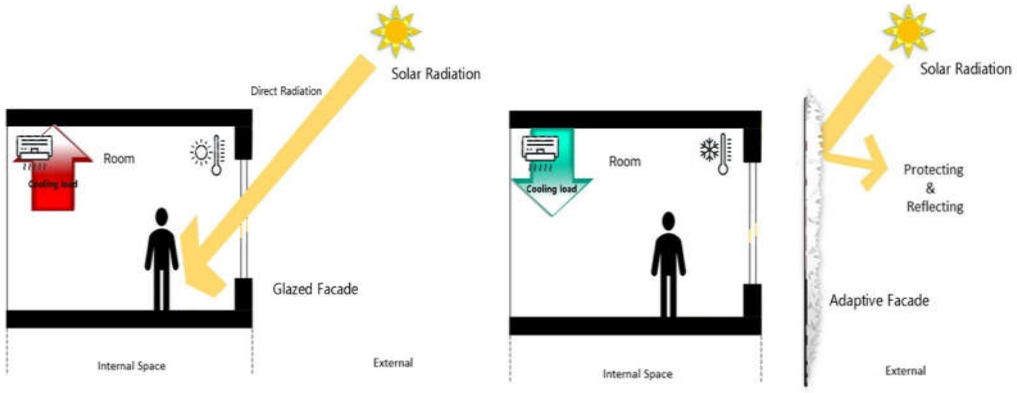

Figure 24. Impact of installing an adaptive façade on heat gain and energy.

On August 24, the results compared the basic model and adaptive facades in the living room and bedroom heat gain(kWh) received. Figure 25 compares the baseline total solar heat gain of 29.9

Preprints (www.preprints.org) | NOT PEER-REVIEWED | Posted: 14 July 2023 doi:10.20944/preprints202307.0931.v1

kWh in the living room and 4.8 kWh in the bedroom and the adaptive facade under the combination scenario. The results show a significant reduction in solar heat gain, with a 98% decrease in 0.5 kWh in the living room and a 79% decrease in 1 kWh in the bedroom. Furthermore, the air temperature scenario results in a reduction of 84% in the living room to 4.6 KWh and 77% in the bedroom to 1.1 KWh, while a solar radiation control scenario results in the lowest reduction of 41% in the living room to 17.4 kWh and no change in the bedroom.

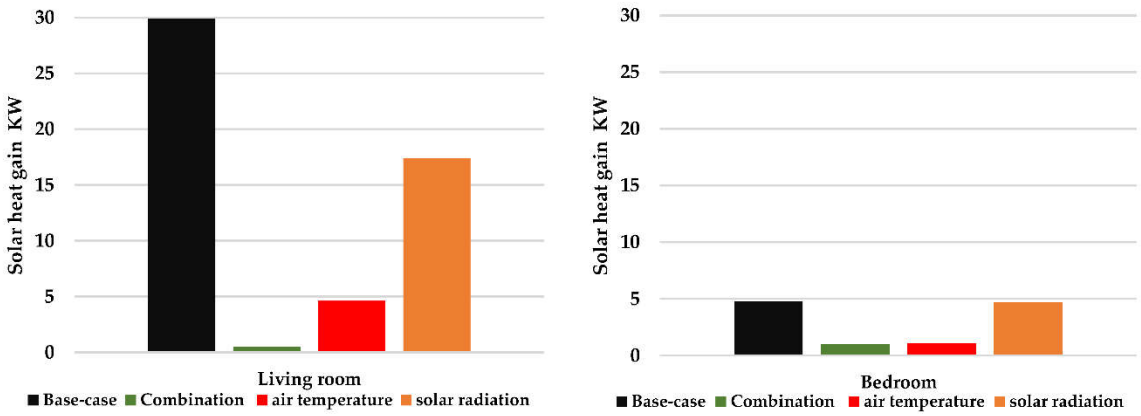

Figure 25. Heat gain in rooms with glazed facade Vs adaptive façade under all scenarios August 24.

Figures 26 and 27 show the impact of annual heat gain from the adaptable façade (MWh) compared to the baseline façade in the living room and bedroom. The combined activation resulted in the most remarkable improvement in the baseline living room and bedroom, followed by the solar radiation technique and the air temperature scenario. Compared to the results of August 24, excessive radiation during the winter months that activated the closed position for an extended time shows that the adaptive facade controlled by solar radiation functions better than the air temperature.

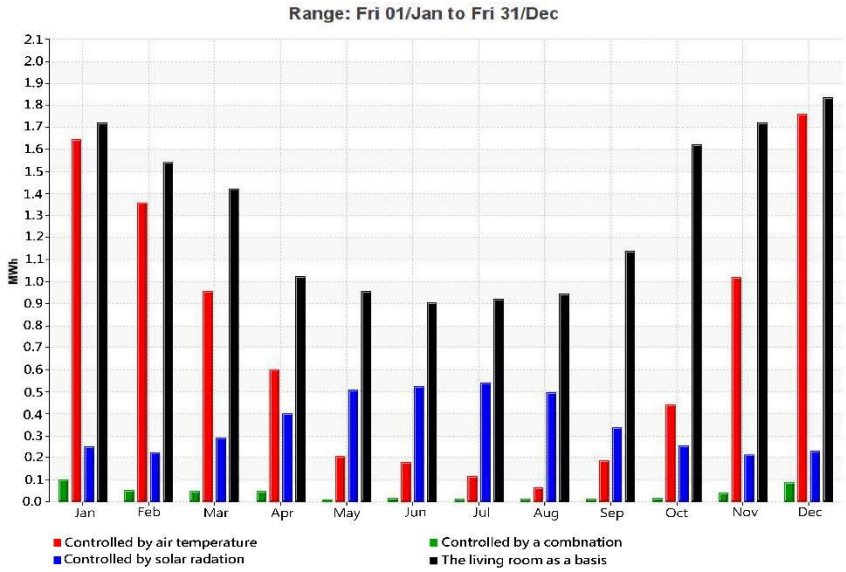

Figure 26. Heat gain in the glazed living room facade Vs adaptive façade under all activations – yearly.

Preprints (www.preprints.org) | NOT PEER-REVIEWED | Posted: 14 July 2023 doi:10.20944/preprints202307.0931.v1

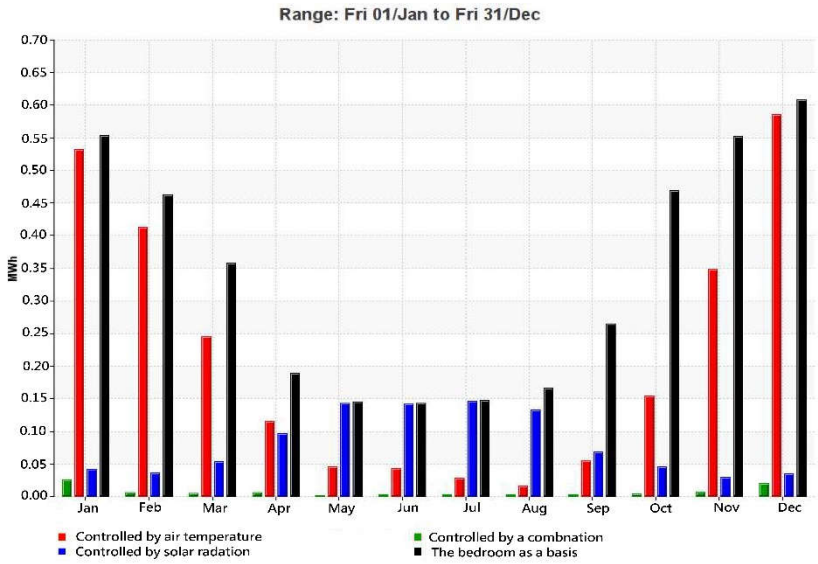

Figure 27. Heat gain in the bedroom glazed facade Vs adaptive façade under all activations – Yearly.

Furthermore, Figure 28 compares the total results of the adapted façade with the glazed facade. The living room received 15.7 MWh, while the bedroom received 4 MWh. The combo scenario reduced the heat of the living room by 97% to 0.5 MWh and the heat gain of the bedroom by 97.5% to 0.1 MWh. Furthermore, the solar radiation scenario reduced the heat in the living room by 73% to 4.2 MWh and in the bedroom by 93% to 1 MWh, while the control of air temperature reduced it by 45% to 8.5 MWh and 37% to 2.5 MWh, respectively.

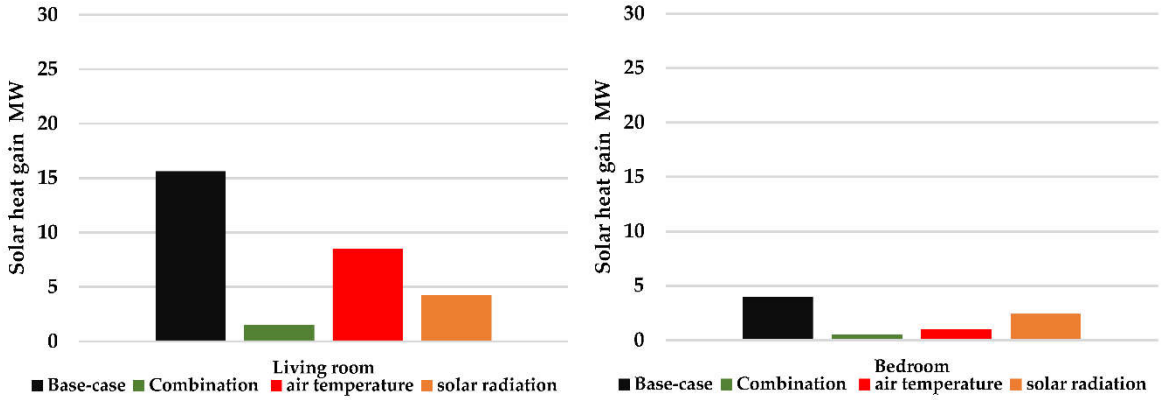

Figure 28. Total heat gain in the glazed facade Vs adaptive façade under all activations – Yearly.

4.3.2. Energy use and cooling

Energy savings in hot climates are primarily based on cutting down on cooling demand to keep the interior comfortable. Based on the simulation results, the adaptive facade shading system has decreased the solar heat gain and indoor temperature and consequently decreased the cooling load and total energy usage. On August 24, the results showed that adaptive façade control under all activation scenarios significantly reduced cooling loads compared to the baseline facade. Furthermore, the adaptive facade activated by the combination resulted in the most significant cooling reduction in the baseline living room and bedroom, followed by the activation of the air temperature, and then the activation of the solar radiation with the lowest drop.

On August 24, Figure 29 compares the cooling loads of the adaptive glazed facades activated by various environmental variables in the living room and bedroom. The result showed that the living room with a glazed facade requires 59.3 kWh of cooling load compared to the adaptive façade activated by the combination, which reduced this by 38 % to 36.7 kWh. Using only air temperature

Preprints (www.preprints.org) | NOT PEER-REVIEWED | Posted: 14 July 2023 doi:10.20944/preprints202307.0931.v1

control reduced this by 29%, bringing the total down to 42.1 kWh; under the solar radiation scenario, the cooling load is reduced by 21% to 46.8 kWh. In contrast, the bedroom with a glazed facade has a cooling demand of 34.2 kWh compared to the adaptive façade controlled by the combination activator, reducing the cooling load to 24.2 kWh, representing a 29% reduction. Using a temperature control strategy decreased the bedroom's cooling load by 21%, resulting in a total of 27.1 kWh. However, in the solar radiation activator scenario, the cooling load was reduced by 15% to reach 29 kWh.

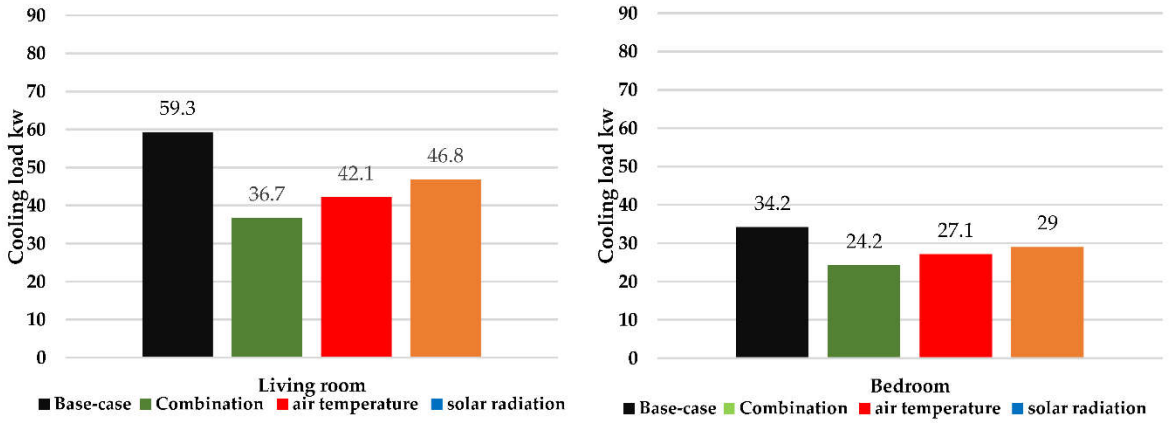

Figure 29. Cooling load in the glazed facade Vs adaptive façade under all activations – August 24.

However, Figure 30 shows the difference in annual cooling load(kWh) between the baseline and adaptive facades in the living room and bedroom. The adaptive system activated by integrating parameters leads to the most significant reduction in cooling demand in the living room and the bedroom; second comes the solar radiation parameter and the last is the activation of the air temperature.

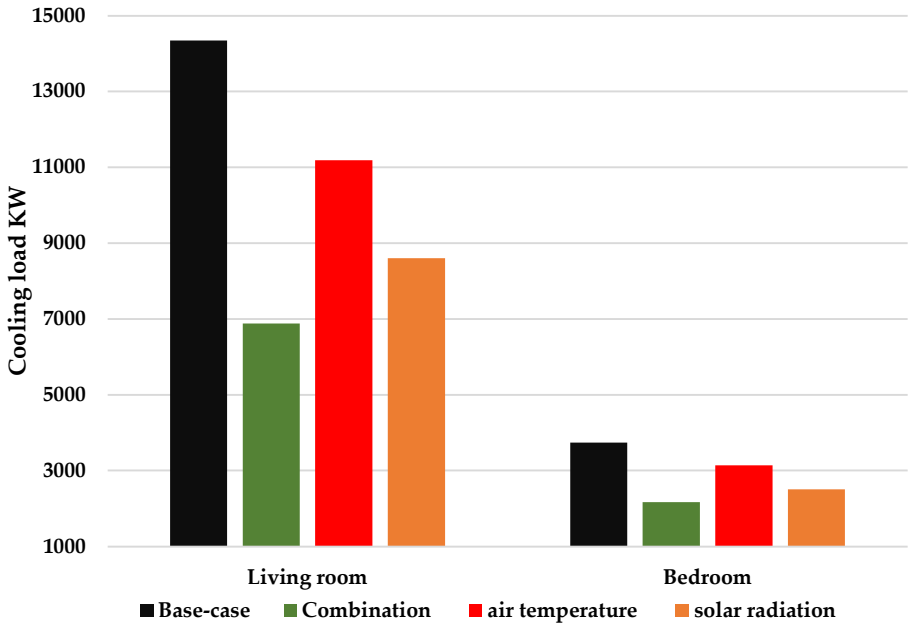

Figure 30. Cooling load in glazed facade Vs adaptive façade under all activations – Yearly.

The results showed that the cooling load of the living room was annually 14,343 kWh on the base façade compared to the adaptive system under combination control, having the highest reduction of 52%, resulting in a cooling load of 6,882 kWh. The solar radiation scenario drops to 8,605 kWh, a decrease of approximately 40%, while the air temperature scenario reduces the cooling load by 22% to 11,185 kWh. However, the cooling usage in the bedroom was annually 3,742 kWh with a glazed façade. Compared to the existing facade, the adaptive system with combination control cut the

Preprints (www.preprints.org) | NOT PEER-REVIEWED | Posted: 14 July 2023 doi:10.20944/preprints202307.0931.v1

cooling load by 42%, leading to a total cooling load of 2,170 kWh. However, solar radiation control reduces the cooling load to 2,507 kWh, which is a reduction of 33%, while the air temperature scenario lowers the cooling load by 16% to 3.140 kWh.

Implementing the adaptive facade shading system that responds to changing weather conditions has reduced the total energy consumption of apartment rooms, including cooling and lighting. The results of the annual study indicated that when a combination of variables activates the adaptive facade, this results in significant total energy savings by optimally minimising the cooling load, but slightly increasing the usage of light. In contrast, the solar radiation scenario reduced the total energy consumption related to lighting energy as a result of improving the apartment's daylighting condition, which reduces the reliance on artificial lighting sources.

In the living room, the total annual energy consumption, including cooling and lighting, was 15,815 kWh with a glazed façade compared to the implementation of the adaptive facade governed by the combination scenario, the energy consumption decreased significantly to 8,132 kWh by 48 %. Furthermore, the solar radiation scenario reduced total energy by 43%, from 15,815 to 9,014 kWh, while the air temperature scenario was reduced by 20% to 12,654 kWh. In contrast, in the bedroom, the total annual energy consumption, including cooling and lighting, was 4.092 kWh with a glazed facade compared to the adaptive system with a 40% reduction in combination control, resulting in a consumption of 2,460 kWh. Furthermore, solar radiation control reduced the overall energy to 2,682 kWh, which is a reduction of 34.4%, while the air temperature scenario reduces the general power by 15 % to 3,471 kWh.

Figure 31 represents a notable enhancement in the adaptive façade activation by merging solar radiation and air temperature. This improvement results in an overall reduction in energy use of approximately 7683 kWh, about 39%. As a result, this energy savings measure effectively decreases carbon emissions by approximately 3,800 kg, substantially contributing to environmental sustainability by lowering the demand for electricity generated from fossil fuels.

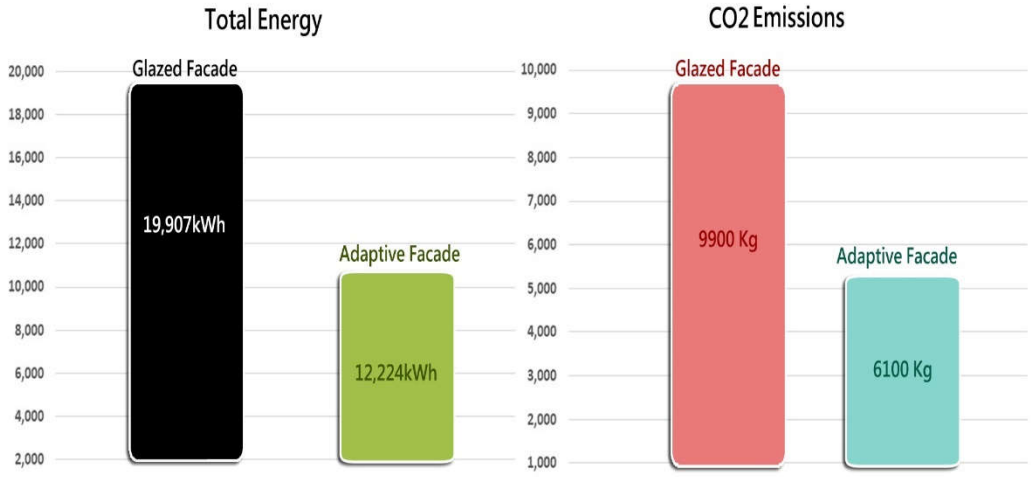

Figure 31. Annual energy savings and CO2 emissions, glazed facade Vs adaptive facade activated by combined variables.

5. Discussion

This study aims to find the optimal thermal activation parameters for the SMP actuator to improve the performance of adaptable façades in a hot-humid climate by examining and analysing the impacts of various SMP activation settings on energy efficiency and occupant comfort and daylighting. Based on all findings from the various design parameters, including air temperature, solar radiation, and the combination in the operation of the adaptive facade with an SMP actuator, this can offer a valuable understanding of the potential to improve the overall performance of the adaptive

 doi:10.20944/preprints202307.0931.v1

façade system. The results found that the operating schedule of the adaptive shading system, which depends on the thermal threshold for SMP activation, plays a critical role in its overall performance.

On August 24, this study evaluated the effects of various thresholds on occupant comfort and energy efficiency. Using a single activation, such as a 33 ° C air temperature threshold, operating the system for 17 hours in a closed position was not sufficient to achieve the ideal balance between comfort for the occupant and daylight performance. Similarly, relying solely on a solar radiation threshold of 275 W/m², enabling the system to respond to intense sunlight for 4 hours, also failed to meet comfort but improved visual comfort. However, combining these thresholds identified an optimal operating schedule that achieved the desired balance of comfort for the occupant and energy savings in 8 hours of function. Thus, the triggered adaptive system provides effective shading during the needed periods and mitigates glare when the solar radiation is intense.

The result of optimal operation under combined activation showed that dynamic shading was closed for approximately 8 hours between 8:00 am and 4:00 pm, which reduced direct sunlight, solar gain, and radiant temperature, reduced the average indoor temperature by 4.9 ° C and 3.6 ° C in the living room and bedroom, respectively, and improved thermal comfort for 4 hours in the living room and 2 hours in the bedroom, saving energy by decreasing the cooling power in the living room from 218 kWh to 135 kWh by 38% and the bedroom from 34.2 kWh to 24.2 kWh by 29%. Furthermore, it reduced the glare of the room to 26.25% (DGP), less than 35%, indicating imperceptible and improving visual comfort. However, it is important to note that the adaptive system in a combined scenario requires artificial lighting for up to 50% of the room space.

However, to make the right decision and understand how the factors affect the interior performance, compare the annual simulation results of the baseline and adaptive facades under various activation parameters. Therefore, this work uses evaluation tools to determine the optimal parameter control strategies that meet the required criteria and sub-criteria. The multi-criteria decision-making method (MCDM) assesses thermal comfort, energy efficiency, and visual comfort for adaptive facade shading systems. This method is based on a structured hierarchy of criteria and sub-criteria or objectives [50] relevant to the evaluation of the performance of adaptive façade systems. The model uses the comparisons and weights of each criterion and sub-criterion and their performance on a set of benchmarks to choose the most effective scenario.

The main criteria considered in this study are energy efficiency, thermal comfort, and visual comfort. The significance of these criteria was determined by prioritising the objectives of this study, which aligns with the Saudi vision [8] of reducing cooling energy consumption, improving thermal comfort, and promoting sustainable practises, while lighting energy accounts for less of the overall energy use. The weights assigned to each criterion are as follows: energy efficiency is the most important, followed by thermal comfort and visual comfort, which are as follows:

1. Energy Efficiency Criterion; the value is 50%, including a reduction of solar heat gain by 15%, a minimisation of cooling loads by 20%, a reduction of overall energy consumption by 10%, and a reduction of carbon emissions by 5%.
2. Thermal Comfort Criterion; it is 30%, including reducing the indoor temperature by 15% and minimising cooling loads by 15%.
3. Visual Comfort Criterion; it is 20%, including daylighting optimisation by 10% and reduction of glare by 10%.

This method identifies key activation parameters that significantly impact the overall thermal performance of SMP-based adaptive shading systems. The total weights are calculated for each criterion and subcriterion to evaluate the efficiency of these parameters. Table 6 summarises the results of the overall performance calculations made using Formula (3):

$$\text{(subcriteria weight) x (result percentage) / 100} \quad (3)$$

For example, consider the indoor temperature reduction subcriterion with a weight of 15% and an annual result percentage of 25%. The calculation would be (15%) x (25%) / 100 = 0.0375, indicating a contribution of 3.75% out of 15% of the total weight of the indoor temperature reduction criterion.

Preprints (www.preprints.org) | NOT PEER-REVIEWED | Posted: 14 July 2023 doi:10.20944/preprints202307.0931.v1

Table 6. The general performance of the adaptable façade under all activation parameters.

Space	Criteria	Sub-Criteria	Air Temperature	Solar Radiation	Combining both
Living Room	**Energy Efficiency 50%**	Reduction of solar heat gain	6.7	10.9	14.5
		Minimisation of cooling load	4.4	8	10.4
		Reduction overall energy (Cooling+ Lighting)	2	4.3	4.8
		Lower carbon emissions	1	2.1	2.4
	Total		14.1%	25.3%	32.1%
	Thermal Comfort 30%	Reduction of indoor temperature	0	0.9	2.4
		Reduction of discomfort hours	0	3.9	7.6
	Total		0%	4.8%	10%
	Visual Comfort 20%	Reduction of glare	7	6	7
		Optmasiton of daylighting	2	4.5	2
	Total		9%	10.5%	9%
Overall performance			**23.1%**	**40.6%**	**51.1%**

According to Table 6, the annual evaluation indicated that the combined scenario is the most successful way of activating to increase the performance of the adaptive facade shading system throughout the seasons, achieving the highest score of 51.1%, followed by solar radiation activation at 40.6%, and the lowest activation is achieved by the temperature at 23.1%. Furthermore, this scenario effectively balances energy efficiency and comfort by reducing heat gain and cooling load and improving indoor thermal and visual comfort conditions. Energy efficiency demonstrated the most significant improvement among the performance criteria, followed by thermal and visual comfort. Specifically, the enhancements achieved an impressive 32.1% out of 50% in the energy efficiency criteria, resulting in a remarkable 10.4%out of 20% reduction in cooling load, representing 52% of the subcriteria. However, it should be noted that there was a slight increase in lighting energy usage of 4%. Therefore, it resulted in an overall energy saving of 48%.

The overall thermal comfort criterion improved by 66.6%, representing a remarkable 10% of 30%. The average interior temperature was lowered by 6 °C, significantly reducing discomfort hours by 49%. However, visual comfort performance demonstrated a significant 70% decrease in glare. However, it did not optimise the distribution of natural light throughout the space, requiring artificial lighting in half of the room.

The variation in the effectiveness of the system when activated by air temperature or solar radiation can be attributed to the specific weather conditions in Jeddah. The solar radiation activator performs significantly better throughout the year because the Sun's path is shifting to the south, aligning with the apartment's orientation. This allows the adaptive shading system to effectively block intense solar radiation and reduce heat gain, resulting in improved performance. However, the air temperature activator performs better during the summer months because it considers the high outdoor temperatures during that time. The system can efficiently respond to the hot climate by closing the shading devices and minimising heat gain. However, during the winter months, the outdoor temperatures in Jeddah are relatively low, causing them to fall below the activation threshold of the adaptive shading system. As a result, shading devices remain open for longer periods, limiting their ability to effectively prevent heat gain. These findings suggest that the solar radiation activator is more influential than the air temperature in optimising visual comfort and reducing lighting energy, as solar radiation is a dominant factor in the climate of Jeddah.

Determining the optimal activation parameters for the adaptive shading system, which depends on the SMP actuator, requires considering various elements such as the local climate, the orientation of the building, and the particular performance goals of the adaptable facade. The combination of

solar radiation and air temperature appears to be the most relevant climatic parameter for triggering the system's reaction to changing weather conditions in Jeddah, Saudi Arabia. This combination of parameters minimises solar gain and cooling load, resulting in energy savings and better occupant comfort. The selection of these precise parameters is critical to obtaining optimal performance and increasing the overall efficacy of the adaptive shading system.

6. Conclusions

The implementation of a thermoresponsive SMP actoutor based-adaptive shading system aims to achieve functionality and efficiency goals in building design. This study investigated the effectiveness of the activation parameters of the system to optimise energy efficiency and improve thermal and visual comfort. Various activation scenarios were evaluated through extensive simulations of IES-VE software, including solar radiation-based operation, air temperature-based operation, and combined solar radiation and air temperature-based operation. In August, the hottest month, Nicol's adaptive comfort approach, which found the suitable comfort limit range for the investigation, was used to determine the air temperature threshold at 33 ° C and the average direct solar radiation defined as the threshold of 275 W/m2. The combination-based activation proved the most effective, allowing the adaptive facades to respond dynamically and adjust to weather fluctuations. On average, the adaptive facades operated for 8 hours, effectively reducing solar heat gain, optimising daylighting, enhancing thermal comfort, and saving energy. On the hottest day, the system achieved a reduction of 6 ° C in the mean indoor temperature and improved hours of thermal comfort, significantly reducing cooling energy. Implementing this energy-conserving approach results in a significant annual reduction of approximately 39% in energy consumption and a decrease of 3,800 kg of CO2 emissions.

This study has certain limitations. The evaluation of daylighting performance was limited due to the lack of an operational profile control feature within the IES-VE software, which only applies to thermal calculations and excludes daylighting simulation. Furthermore, the physical behaviour of the SMP actuators could not be included in the study due to the lack of material properties in the simulation software. Thus, simulating the performance of SMPs poses challenges in capturing their reaction time, reversible deformation, and temperature-dependent behaviours. Future research should focus on scaling up the implementation of adaptive facades in real-world contexts to assess their long-term performance. Alternative simulation tools or a combination of tools should be explored to assess the thermal response of SMP materials. Continuous monitoring and feedback from occupants can help refine the system's operation and strike a balance between comfort and energy efficiency. In addition, incorporating natural or mechanical ventilation calculations can optimise thermal comfort and overall building performance.

Author Contributions: M.Z. is the principal author. P.B. and C.W. contributed to writing: review and editing, and supervision. All authors have read and agreed to the published version of the manuscript.

Funding: This research did not receive external funding.

Conflicts of Interest: The authors declare that they have no conflict of interest.

References

1. N. Ghabra, L. Rodrigues, and P. Oldfield, "The impact of the building envelope on the energy efficiency of residential tall buildings in Saudi Arabia," *Int. J. Low-Carbon Technol.*, vol. 12, no. 4, pp. 411–419, 2017, doi: 10.1093/ijlct/ctx005.
2. A. Kamal *et al.*, "Detailed profiling of high-rise building energy consumption in an extremely hot and humid climate," *Clean. Energy Syst.*, vol. 4, no. February, p. 100060, 2023, doi: 10.1016/j.cles.2023.100060.
3. N. Nazarian *et al.*, "Integrated Assessment of Urban Overheating Impacts on Human Life," *Earth's Futur.*, vol. 10, no. 8, 2022, doi: 10.1029/2022EF002682.
4. J. Duan, N. Li, J. Peng, C. Wang, Q. Liu, and X. Zhou, "Study on occupant behaviour of air conditioning of high-rise residential buildings in hot summer and cold winter zone in China," *Energy Build.*, vol. 276, p. 112498, 2022, doi: 10.1016/j.enbuild.2022.112498.
5. K. J. Lomas and S. M. Porritt, "Overheating in buildings: lessons from research," *Build. Res. Inf.*, vol. 45, no. 1–2, pp. 1–18, 2017, doi: 10.1080/09613218.2017.1256136.

6. A. Felimban, A. Prieto, U. Knaack, T. Klein, and Y. Qaffas, "Assessment of current energy consumption in residential buildings in Jeddah, Saudi Arabia," *Buildings*, vol. 9, no. 7, 2019, doi: 10.3390/buildings9070163.
7. Ministry of Housing, "Mostadam Rating System for Residential Buildings D + C," p. 4, 2019, [Online]. Available: https://www.mostadam.sa/uploads/2019/09/5d91b53e0b866.pdf.
8. K. Salman, B. I. N. Abdulaziz, and A. L. Saud, "Saudi Vision 2030," 2016. https://www.vision2030.gov.sa/ (accessed Jan. 20, 2023).
9. H. Han, "Governance for green urbanisation: Lessons from Singapore's green building certification scheme," *Environ. Plan. C Polit. Sp.*, vol. 37, no. 1, pp. 137–156, 2019, doi: 10.1177/2399654418778596.
10. B. Koch, J., Schopfer, J., & Schmitz, "Dynamic shading systems in high-rise office buildings — Potential for energy savings and thermal comfort improvement," *Energy Build.*, p. 43(9), 2011.
11. D. Aelenei, L. Aelenei, and C. P. Vieira, "Adaptive Façade: Concept, Applications, Research Questions," *Energy Procedia*, vol. 91, pp. 269–275, 2016, doi: 10.1016/j.egypro.2016.06.218.
12. R. C. G. M. Loonen, M. Tr, D. Cóstola, and J. L. M. Hensen, "Climate adaptive building shells : state-of-the-art and future challenges," vol. 25, pp. 483–493, 2013.
13. A. Sandak, *Bio-based Building Skin*. Springer Open, 2019.
14. R. C. G. M. Loonen, "Overview of 100 Climate Climate Adaptive Building Shells," no. 2010, p. 106, 2010, [Online]. Available: https://pure.tue.nl/ws/portalfiles/portal/15945980/Loonen2010_OverviewOf100ClimateBuildingShells.
15. D. K. Bui, T. N. Nguyen, A. Ghazlan, N. T. Ngo, and T. D. Ngo, "Enhancing building energy efficiency by adaptive façade: A computational optimization approach," *Appl. Energy*, vol. 265, no. March 2020, doi: 10.1016/j.apenergy.2020.114797.
16. S. Attia, *Regenerative and positive impact architecture : Learning from case studies*. New York City, 2018.
17. F. Favoino, R. C. G. M. Loonen, M. Doya, F. Goia, C. Bedon, and F. Babich, "Building Performance Simulation and Characterisation of Adaptive Facades-Adaptive Facade Network," Jan. 2018.
18. H. Schnadelbach, A. Penn, S. Benford, and B. Koleva, "Mixed Reality Architecture: Concept, Construction, Use," *Tech. Rep. Equator Univ. Nottingham Nottingham*, pp. 1–27, 2003.
19. S. Jain and V. Garg, "A review of open loop control strategies for shades, blinds and integrated lighting by use of real-time daylight prediction methods," *Build. Environ.*, 2018, doi: 10.1016/j.buildenv.2018.03.018.This.
20. J. Yoon, "SMP Prototype Design and Fabrication for Thermo-responsive Façade Elements," *J. Facade Des. Eng.*, vol. 7, no. 1, pp. 41–61, 2019, doi: 10.7480/jfde.2019.1.2662.
21. I. N. Qader, M. Kok, F. Dagdelen, Y. Aydogdu, and I. N. Qader, "A Review of Smart Materials: Researches and Applications," *El-Cezerî J. Sci. Eng.*, vol. 6, no. 3, pp. 755–788, 2019, [Online]. Available: www.dergipark.gov.tr.
22. S. Mumme, N. James, M. Salonvaara, S. Shrestha, and D. Hun, "Smart and efficient building envelopes: Thermal switches and thermal storage for energy savings and load flexibility," *ASHRAE Trans.*, vol. 126, pp. 140–148, 2020.
23. A. Battisti, S. G. L. Persiani, and M. Crespi, "Review and mapping of parameters for the early stage design of adaptive building technologies through life cycle assessment tools," *Energies*, vol. 12, no. 9, 2019, doi: 10.3390/en12091729.
24. R. Neuhaus *et al.*, "Integrating Ionic Electroactive Polymer Actuators and Sensors Into Adaptive Building Skins – Potentials and Limitations," *Front. Built Environment*, vol. 6, no. July, pp. 1–22, 2020, doi: 10.3389/fbuil.2020.00095.
25. C. Liu, H. Qin, and P. T. Mather, "Review of progress in shape-memory polymers," *J. Mater. Chem.*, vol. 17, no. 16, pp. 1543–1558, 2007, doi: 10.1039/b615954k.
26. J. Li, Q. Duan, E. Zhang, and J. Wang, "Applications of shape memory polymers in kinetic buildings," *Advances in Materials Science and Engineering*, vol. 2018. Hindawi Limited, 2018, doi: 10.1155/2018/7453698.
27. J. Yoon and S. Bae, "Performance evaluation and design of thermo-responsive SMP shading prototypes," *Sustain.*, vol. 12, no. 11, 2020, doi: 10.3390/su12114391.
28. S. Imai, "Operating methods for two-way behavior shape memory polymer actuators without using external stress," *IEEJ Trans. Electr. Electron. Eng.*, vol. 9, no. 1, pp. 90–96, 2014, doi: 10.1002/tee.21940.
29. S. Beites, "Morphological behavior of shape memory polymers toward a deployable, adaptive architecture," *ACADIA 2013 Adapt. Archit. - Proc. 33rd Annu. Conf. Assoc. Comput. Aided Des. Archit.*, pp. 121–128, 2013.
30. H. Alkhatib, P. Lemarchand, B. Norton, and D. T. J. O'Sullivan, "Deployment and control of adaptive building facades for energy generation, thermal insulation, ventilation and daylighting: A review," *Appl. Therm. Eng.*, vol. 185, no. November, p. 116331, 2021, doi: 10.1016/j.applthermaleng.2020.116331.
31. A. Tabadkani, A. Roetzel, H. X. Li, and A. Tsangrassoulis, "Design approaches and typologies of adaptive facades: A review," *Autom. Constr.*, vol. 121, no. November 2020, p. 103450, 2021, doi: 10.1016/j.autcon.2020.103450.

32. S. Bonser, A. Kuru, P. Oldfield, S. Bonser, and F. Fiorito, "Biomimetic adaptive building skins : Energy and environmental regulation in buildings Energy & Buildings Biomimetic adaptive building skins : Energy and environmental regulation in buildings," *Energy Build.*, vol. 205, no. October, p. 109544, 2019, doi: 10.1016/j.enbuild.2019.109544.
33. G. Yun, D. Y. Park, and K. S. Kim, "Appropriate activation threshold of the external blind for visual comfort and lighting energy saving in different climate conditions," *Build. Environ.*, vol. 113, pp. 247–266, 2017, doi: 10.1016/j.buildenv.2016.11.021.
34. G. Evola, F. Gullo, and L. Marletta, "The role of shading devices to improve thermal and visual comfort in existing glazed buildings," *Energy Procedia*, vol. 134, pp. 346–355, 2017, doi: 10.1016/j.egypro.2017.09.543.
35. M. H. Oh, K. H. Lee, and J. H. Yoon, "Automated control strategies of inside slat-type blind considering visual comfort and building energy performance," *Energy Build.*, vol. 55, pp. 728–737, 2012, doi: 10.1016/j.enbuild.2012.09.019.
36. A. Nezamdoost, K. Van Den Wymelenberg, and A. Mahic, "Assessing the energy and daylighting impacts of human behavior with window shades, a life-cycle comparison of manual and automated blinds," *Autom. Constr.*, vol. 92, no. April, pp. 133–150, 2018, doi: 10.1016/j.autcon.2018.03.033.
37. C. I. of B. S. Engineers, *Chartered Institution of Building Services Engineers (CIBSE). Guide A: Environmental Design*, 8th ed. London, UK, 2015.
38. Passive House Institute, "Criteria for Buildings Passive House – EnerPHit –PHI Low Energy Building," no. January, [Online]. Available: www.passivehouse.com.
39. M. of Housing, "Mostadam Rating System Residential Buildings D+C Manual," 2019.
40. A. N. Alnuaimi and S. Natarajan, "The energy cost of cold thermal discomfort in the global south," *Buildings*, vol. 10, no. 5, 2020, doi: 10.3390/BUILDINGS10050093.
41. R. Elnaklah, A. Alnuaimi, B. S. Alotaibi, E. Topriska, I. Walker, and S. Natarajan, "Thermal comfort standards in the Middle East: Current and future challenges," *Build. Environ.*, vol. 200, no. May, p. 107899, 2021, doi: 10.1016/j.buildenv.2021.107899.
42. A. Andersen *et al.*, "Daylight, Energy and Indoor Climate Basic Book," no. December, p. 150, 2014, [Online]. Available: http://www.velux.com/~/media/com/articles/pdf/deic_basic_book_ver 3-0.pdf.
43. S. Szokolay, *Introduction to ARCHITECTURAL SCIENCE the basis of sustainable design*, 3rd Editio. London, 2014.
44. Saudi Energy Efficiency Center, "Annual Report 2021," 2021. https://www.seec.gov.sa/en/media-center/annual-report/.
45. A. M. Shatwan, "Domestic Window Design and Interior Daylight in Jeddah : Designing for Saudi Women Doctor of Philosophy," 2018.
46. CEN, "CEN European Daylight Standard (EN 17037), Daylighting in building," 2018, Google Scholar.
47. D. B. Crawley, J. W. Hand, M. Kummert, and B. T. Griffith, "Contrasting the capabilities of building energy performance simulation programs," *Build. Environ.*, vol. 43, no. 4, pp. 661–673, 2008, doi: 10.1016/j.buildenv.2006.10.027.
48. M. Alwetaishi, "Impact of glazing to wall ratio in various climatic regions: A case study," *J. King Saud Univ. - Eng. Sci.*, vol. 31, no. 1, pp. 6–18, 2019, doi: 10.1016/j.jksues.2017.03.001.
49. ASHRAE, *Pocket Guide for Air Conditioning, Heating, Ventilation, refrigeration*, 9th ed. W. Stephen Comstock, 2017.
50. K. Y. Ching-Lai Hwang, *Methods for Multiple Attribute Decision Making*. Berlin: Springer, 1981.